Herpetological Monographs, 35, 2021, 000–000

Analysis of Bobbing Displays in the *Grahami* Series Anoles from Jamaica and Grand Cayman

Joseph M. Macedonia[1,4], David L. Clark[2], and Morgan R. Fonley[3]

[1] Department of Biology, Florida Southern College, Lakeland, FL 33801, USA
[2] Department of Biology, Alma College, Alma, MI 48801, USA
[3] Department of Mathematics, Alma College, Alma, MI 48801, USA

Abstract: Behavioral biologists have long been fascinated with the diversity of animal signals produced in the contexts of courtship and same-sex competition. In these contexts many lizards engage in conspicuous bobbing displays, and numerous studies have been devoted to describing these displays. Traditionally, bobbing displays are partitioned into units whose durations (and sometimes head amplitudes) are measured. Recently, Macedonia et al. (2019) introduced use of the Discrete Fourier Transform (DFT) as an alternative to unit-based variables for characterizing species-specific traits in display structure of Galápagos Lava Lizards (*Microlophus* spp.). The relative success of the two methods was not compared directly, however, because the homology of display units among species was uncertain. Here we overcome this problem using the "*grahami* series" of *Anolis* lizards—a monophyletic radiation of seven species on Jamaica and Grand Cayman. Our study had three primary goals. Our first goal was to discover whether DFT-based measures, unit-based measures, or their combination provided the best means to capture taxon-specific distinctiveness in display structure. To this end, we quantified bobbing displays and used nested analyses of variance (ANOVAs) to determine if particular variables were reliably superior at differentiating populations within a species. We then used principal components analysis to reduce the number of measurement variables, and entered the components into discriminant function analyses to determine which approach best discriminated among taxa. Results showed that no one type of measurement, or measurement combination, emerged as being consistently better at discriminating taxa across comparisons. Our second goal was to test a hypothesis that arose from our findings in Galápagos Lava Lizards—that the DFT may decrease in effectiveness as bobbing display structure increases in complexity. For this test we used four simple and compound display types from the species *Anolis reconditus*. Results of discriminant function analyses provided mixed support for the hypothesis, and we suggest that a definitive test of DFT performance and display complexity should utilize synthetic displays in which attributes of display structure are varied systematically. Last, we show how bobbing display structure maps onto alternative DNA-based phylogenies of the *grahami* series anoles. Whereas some species produced derived display types unanticipated from displays of more basal species in this adaptive radiation, others exhibited features that linked them to a particular population of a species in their clade.

Key words: *Anolis*; Headbob displays; Phylogeny reconstruction; *Placopsis*

Motion displays are widespread in animals and often appear to have evolved as ritualized behaviors that are exhibited during interactions with conspecifics or predators (Bradbury and Vehrencamp 2011). Such signals are particularly common in courtship (Prum 1994; Clark et al. 2017), competition for mates (Clutton-Brock and Albon 1979; Andersson 1994), and in antipredator behavior (Hasson et al. 1989; Leal 1999; Cooper et al. 2004; Caro 2005). The motion displays of lizards have interested herpetologists and behavioral biologists for many decades (Carpenter and Ferguson 1977; Jenssen 1977a; Martins 1993; Martins and Lamont 1998; Martins et al. 2004). Although many types of lizard visual signals have been studied, including the dewlap display (Williams and Rand 1977; Nicholson et al. 2007; Fleishman et al. 2009; Macedonia et al. 2014; Ord et al. 2015), forelimb circumduction (Carpenter et al. 1970; Jenssen 1979a; Peters and Evans 2003; Vicente 2019), tail waving or lashing (Gorman 1968; Hasson et al. 1989; Ramos and Peters 2017), and frill erection (Shine 1990; Perez-Martinez et al. 2020), the most frequently described displays are termed "pushups" and "headbobs" (henceforth collectively termed "bobbing displays"). These displays are particularly common among families of the suborder Iguania (Johnson et al. 2019). Beginning with Carpenter and Grubitz (1961), bobbing displays have been quantified by partitioning them into units (i.e., discrete periods of motion or pauses between motions) and measuring their durations (Ferguson 1971; Jenssen 1977a). Unfortunately, restricting measurements to unit durations overlooks the changes in head amplitude that constitute bobbing. A few more recent studies therefore have analyzed bob amplitude variation and uniformity to more fully describe display structure (Ord and Martins 2006; Labra et al. 2007; Clark et al. 2015; Vicente 2018).

Recently, Macedonia et al. (2019) introduced use of the Discrete Fourier Transform (DFT) to analyze bobbing displays from four species of Galápagos Lava Lizards (*Microlophus* spp., Tropiduridae). An important advantage of the DFT approach is that the same suite of measures can be used to quantify displays with very different structure, whereas statistical comparisons involving unit-based variables are confined to those display types that share a common set of measurable features. In that study (Macedonia et al. 2019), individual displays were quantified with 13 DFT-based frequency and amplitude variables (Table 1). Many of these measures were correlated and/or nonnormally distributed, so principal components analysis (PCA) was used to derive a smaller set of uncorrelated and normally distributed variables (i.e., principal components) from linearly weighted combinations of the DFT variables. The components then were entered into a canonical linear discriminant function analysis (DFA), as well as its permuted form (pDFA), to determine how successfully the discriminant functions could assign displays to the correct species. Results confirmed that the DFT is an excellent tool for capturing taxon-specific traits of bobbing displays, but it also revealed a potential limitation: in a cross-validation DFA, which is that displays with relatively simple structure were more often assigned to the correct species (*Microlophus*

[4] Correspondence: e-mail, Joe.Macedonia@gmail.com

TABLE 1.—Names and definitions of 13 Discrete Fourier Transform-based variables used to quantify bobbing displays in taxa of the *Anolis grahami* series.

Variable	Variable Name	Definition
1	Principal frequency	Frequency corresponding to peak amplitude
2	Peak frequency	Frequency corresponding to highest amplitude from 0 to 5 Hz
3	Partial sum	Partial sum of amplitudes from 0 to 5 Hz
4	Percentage of sum	Proportion of partial sum of amplitude to total sum amplitude from 0 to 5 Hz
5	Mean amplitude	Mean amplitude from 0 to 5 Hz
6–9	Peak frequency, partial sum, percentage of sum, mean amplitude 5–10 Hz	Same as variables 2–5, but for 5–10 Hz
10–13	Peak frequency, partial sum, percentage of sum, mean amplitude 10–15 Hz	Same as variables 2–5, but for 10–15 Hz

albemarlensis = 96%, *M. grayii* = 92%) than were displays with more complex structure (*M. bivittatus* = 63%, *M. indefatigabilis* = 42%). It remains unknown whether the apparent bias in classification success toward bobbing displays with simpler structure was specific to that study or whether it applies more broadly. Thus, DFT performance should be tested with other lizard taxa whose bobbing displays vary in complexity.

The large genus *Anolis* (nearly 400 species; Losos 2009) offers a diverse landscape for additional testing of the DFT approach to bobbing display analysis. The "*Anolis grahami* series" (henceforth, "*grahami* series") clade of anoles provides an ideal case study. With six species on Jamaica and one on Grand Cayman, this adaptive radiation of arboreal microhabitat specialists (or ecomorphs; Williams 1972, 1983; Losos 2009; Stroud and Losos 2020) is diverse yet small enough to be tractable for multiple comparisons. Moreover, this clade has been shown repeatedly in morphological, electrophoretic, and molecular analyses to be monophyletic (Shochat and Dessauer 1981; Hedges and Burnell 1990; Jackman et al. 2002; Poe et al. 2017)—a crucial factor for tracking changes in bobbing display structure over evolutionary time.

Poe et al. (2017) recently proposed the name *Placopsis* to formally recognize the long-standing but informal *grahami* series nomenclature of Shochat and Dessauer (1981). In this paper we predominantly use *grahami* series to refer to this radiation, but we also use *Placopsis* in an introductory manner. The *grahami* series contains two consistently recognized clades and one additional species whose relationship to the two groups has been debated. First, the *Anolis grahami* group (henceforth "*grahami* group") comprises *A. conspersus* (trunk-crown ecomorph on Grand Cayman), *A. garmani* (crown-giant ecomorph), *A. grahami* (trunk-crown ecomorph), and *A. opalinus* (trunk-crown ecomorph). Second, the *Anolis lineatopus* group (henceforth "*lineatopus* group") consists of *A. lineatopus* (trunk-ground ecomorph) and *A. reconditus* (montane generalist). Last is the species *Anolis valencienni,* a twig ecomorph. Four of the seven species are monotypic and lack subspecies: *A. garmani, A. opalinus, A. reconditus, and A. valencienni*. Each of the remaining three polytypic species contains either two or four recognized subspecies: (1) *A. conspersus conspersus* and *A. c. lewisi* (Grant 1940), (2) *A. grahami grahami* and *A. g. aquarum,* and, (3) *A. lineatopus lineatopus, A. l. merope, A. l. ahenobarbus, and A. l. neckeri* (Underwood and Williams 1959). Although the Cuban Brown Anole (*Anolis sagrei*) has been present on Jamaica for ≥170 yr (Underwood and Williams 1959), molecular genetic and phylogeographic analyses (Jackman et al. 2002; Kolbe et al. 2004; Poe et al. 2017; Reynolds et al. 2020) make clear that this broadly distributed species is introduced not only to Jamaica and other Caribbean Islands, but also to the Americas, Hawaii, Asia and elsewhere (e.g., Bermuda; Stroud et al. 2017).

Although researchers agree that the *grahami* series is monophyletic, studies have reached considerably different conclusions about species relationships within the series. For example, relationships among three members of the *grahami* group—*A. grahami, A. garmani,* and *A. opalinus*—have been particularly problematic (in this example we consider *A. conspersus* to be nested within *A. grahami*). Whereas mtDNA sequences revealed an *A. garmani–A. opalinus* clade, the combination of DNA and allozymic data produced an *A. grahami–A. opalinus* clade (Jackman et al. 2002). Moreover, in two more recent studies the combination of nuclear and mitochondrial DNA recovered an *A. grahami–A. garmani* clade (Pyron et al. 2013; Poe et al. 2017). In these studies, as in others prior to them, the relationship of *A. valencienni* to other *grahami* series species has been regularly disputed.

In our comprehensive study we analyze bobbing displays from every recognized *grahami* series taxon except *A. lineatopus neckeri,* for which we lack observations. Displays from *A. l. neckeri* have, however, been described previously by Jenssen (1977b). We use two phylogenies as alternate working hypotheses: the mtDNA-based phylogeny of Jackman et al. (2002; Fig. 1A), and the combined nuclear and mitochondrial DNA species-level study of Poe et al. (2017), into which we incorporate the subspecies relationships of Jackman et al. 2002 (Fig. 1B). Our overall objectives are as follows. First, we illustrate the physical structure of bobbing displays and describe details of their execution, including the relationship of bobbing to dewlap extension and retraction. Next we quantify unit durations and standardized peak amplitudes in bobbing displays for all but one species (*A. lineatopus;* see below), and provide descriptive statistics for these variables at the species, subspecies, and population levels (see Supplemental Materials available online). We then use nested analyses of variance (ANOVAs) to partition display variance into within-subject, among-subject, and among-population variability for the three polytypic species (*A. conspersus, A. grahami,* and *A. lineatopus*). In this way we can determine whether these species differ in their distributions of display variance, and whether particular variables are superior at distinguishing among subspecies (including populations that are not formally recognized). After reducing our numerous display trait variables with

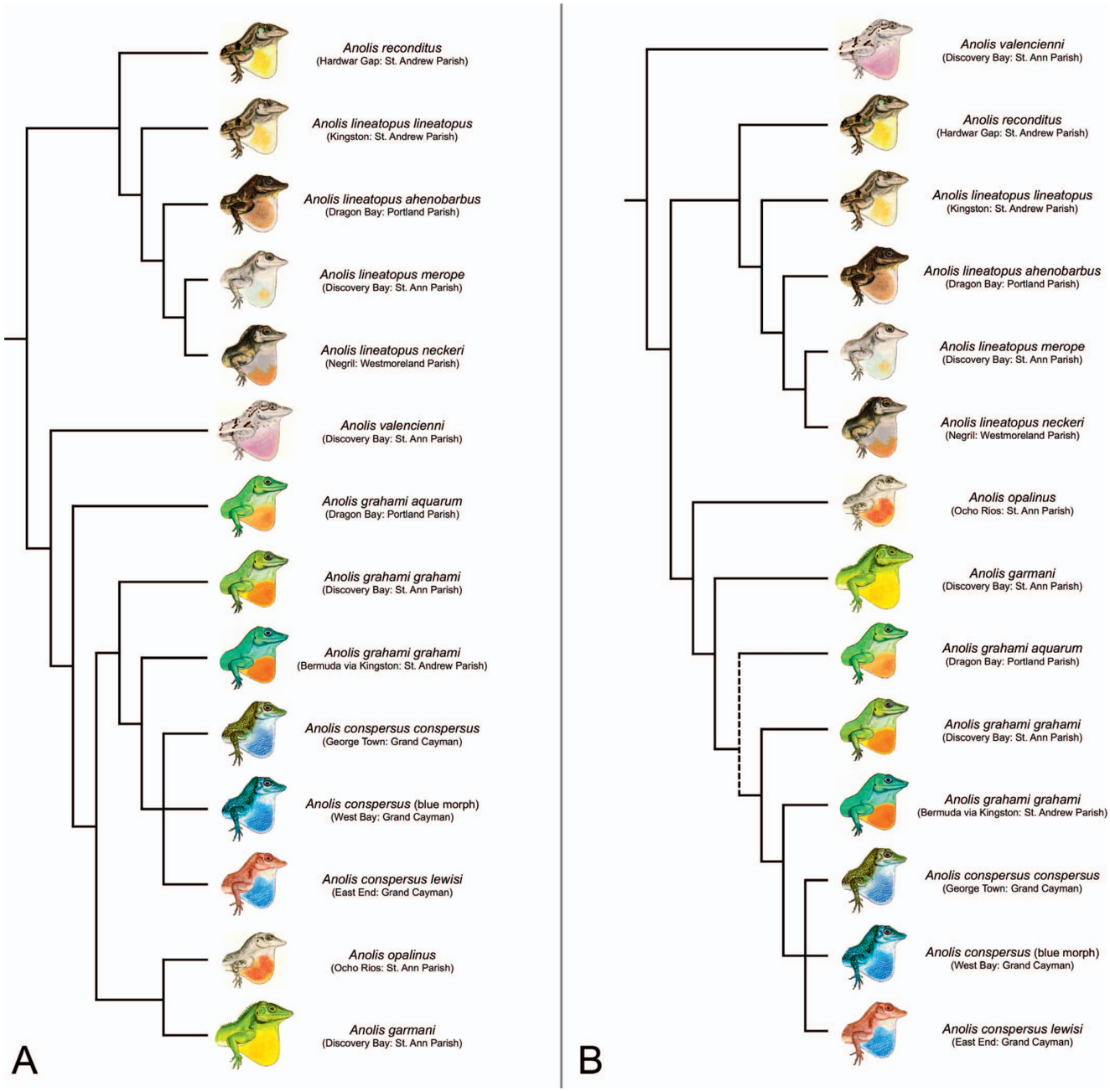

FIG. 1.—Alternative phylogenies of the *grahami* series (*Placopsis)* anoles. (A) Phylogenetic hypothesis of Jackman et al. (2002:fig. 4). In this phylogeny, *Anolis grahami aquarum* shares a common ancestor with the rest of the *grahami* group rather than being a member of an *A. grahami–A. conspersus* clade. (B) Phylogenetic hypothesis of Poe et al. (2017:fig. 3), with intraspecific relationships of Jackman et al. (2002). The dashed line indicates that placement of *A. grahami aquarum* outside an *A. grahami–A. conspersus* clade would violate the species-level results of Poe et al. (2017). The provenance of our study subjects is shown in parentheses under the scientific name of each taxon. In both phylogenies the two recognized *A. conspersus* subspecies are shown in an unresolved trichotomy with a taxonomically unrecognized but widely distributed blue-bodied color morph. Original watercolor illustrations are by David Leber from Schwartz and Henderson (1985), with permission. Coloration in some members of the *A. grahami–A. conspersus* clade has been modified to accurately represent the populations depicted. Coloration of *Anolis reconditus* (not illustrated in Schwartz and Henderson 1985) was adapted from Leber's *A. l. lineatopus* illustration using photos of *A. reconditus* for reference.

PCA, we use both DFA and its permuted form (pDFA) to compare the performance of unit-based and DFT-based variables in correctly assigning displays to the taxon that produced them. Although we cannot make a priori predictions about the relative DFA classification success of unit-based versus DFT-based variables, we offer a prediction based on the findings of Macedonia et al. (2019) for Galápagos Lava Lizard bobbing displays: we predict that classification success of displays measured with DFT variables will decrease as display structure increases in complexity. Finally, in light of our findings we discuss the correspondence between display structure and phylogenetic

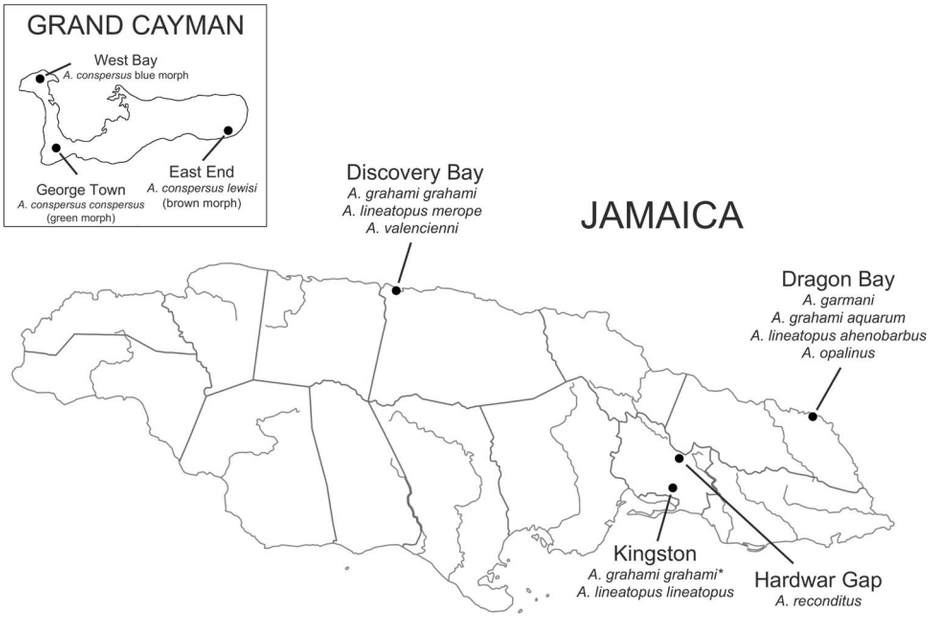

FIG. 2.—Field collection sites with taxa sampled on Jamaica and Grand Cayman. The asterisk following *A. grahami grahami** at Kingston denotes that subjects used in this study were collected in Bermuda and are descendants of individuals transported to Bermuda from Kingston in 1905 (see text).

relatedness among members of the *grahami* series (*Placopsis*) clade of anoles.

MATERIALS AND METHODS

Subjects and Study Areas

Our study subjects were captured by hand or with a pole and snare (made of dental floss, braided suture thread, or fly line backing) that was tied into a running knot. We collected subjects on three islands: Jamaica, Bermuda, and Grand Cayman. On Jamaica we captured lizards at or near the following four locations (Fig. 2): (1) the Discovery Bay Marine Lab, St. Ann Parish, on the north-central coast (*A. grahami grahami, A. lineatopus merope,* and *A. valencienni*), (2) Dragon Bay, Portland Parish, on the northeastern coast (*A. garmani, A. grahami aquarum, A. lineatopus ahenobarbus,* and *A. opalinus*), (3) the Mona, Kingston campus of the University of the West Indies, St. Andrew Parish, in southeast Jamaica (*A. lineatopus lineatopus*), and, (4) along the Fairy Glade trail above Hardwar Gap, Portland Parish, in the Blue Mountains (*A. reconditus*). Underwood and Williams (1959) provided physical descriptions and distribution maps for the six Jamaican species and subspecies; additional coloration accounts of these taxa can be found in Macedonia et al. (2000). Throughout Bermuda we collected *A. g. grahami* subjects that were descendants of a population introduced in 1905 from Kingston, Jamaica (Wingate 1965; Macedonia and Clark 2003). On Grand Cayman we collected (1) *A. conspersus conspersus* (green color morph) in and around George Town, (2) *A. conspersus lewisi* (brown color morph) along the East End Trail, and, (3) a taxonomically unrecognized blue color morph in West Bay in the northwestern part of the island (Fig. 2 inset; see Macedonia 2001 for a collection site map). Although an island-wide survey in the 1930s (Grant 1940) hinted at bluish coloration in some *A. c. lewisi* specimens, there was no mention of a truly blue-bodied morph in the literature prior to Macedonia (2001), despite it having become the most widespread of the color forms at some point between the 1940s and 1980s (Peterson 2016). Descriptions of coloration and distribution maps of *A. conspersus* populations are provided in Macedonia (2001) and Macedonia and Clark (2001). Snout–vent length (SVL) and ecomorph class for all the study subspecies and populations are presented in Supplemental Table S1, available online.

Display Data Collection

Bobbing display data were gathered from video recordings in experimental trials of three types: (1) responses of males to video playbacks of displaying males (Macedonia and Stamps 1994), (2) staged male–male contests or responses of males to a mirror (Macedonia and Clark 2001, 2003), and, (3) responses of males to presentations of conspecific male robots (Macedonia et al. 2013, 2015a). Males and females exhibit the same display structure for displays of the same type (Jenssen 1977a, 1978), although sex differences have been shown for some unit durations in *A. grahami* from Bermuda (Macedonia and Clark 2003). Given that males displayed more frequently than females, and the larger size of males helped facilitate bobbing display data collection from video, with one exception (*A. reconditus*) we included only displays of males in our analyses. We had a small sample size for each sex, so we analyzed data from both sexes of *A. reconditus*. Details of experimental set-ups, hardware and software, and procedural protocols varied across studies and can be found in the aforementioned publications. We did not use any of our previously published data for the present research; all displays used in this study were quantified expressly for this work from the original video recordings.

Jenssen (1977a,b; 1981) initially employed functional terms to describe the contexts in which different bobbing displays were used by *Anolis* species. Displays executed by males while surveying their territories were considered to

occur in the "assertion" context (Carpenter 1962) and were termed Type A displays (also termed "signature" displays; Stamps and Barlow 1973). A display variant that was only observed when conspecific males were engaged in a display contest, termed the "challenge" context (Carpenter 1962), was labeled the Type B display. DeCourcy and Jenssen (1994) later argued for the dissolution of functional terminology for display contexts, in the light that potential future discovery of new functions would cause unnecessary complications. These authors suggested instead that contexts be referred to as male-alone (formerly assertion), male–male (formerly challenge), and male–female (formerly courtship). Note that whereas Type B displays are only performed in the male–male context, Type A displays occur in all three contexts (Jenssen 1981).

In anoles, as in many types of lizards, bobbing displays are produced singly as well as in volleys (i.e., display series; Jenssen 1977a). With one exception (*A. conspersus* Type B displays), we follow DeCourcy and Jenssen (1994) in defining a display volley as a series of two or more displays with interdisplay intervals of <2 s. For *A. conspersus* Type B displays, which are produced only in volleys, we define a volley as two or more displays with interdisplay intervals ≤1 s.

Following Jenssen's (1981) restriction of unit duration measurements to the first nine units in Type A and B displays of *A. grahami* and *A. garmani,* we measured unit durations and standardized peak amplitudes for the first nine display units in *A. grahami, A. garmani, A. opalinus,* and in Type A displays of *A. conspersus*. We required at least seven units (four bobs) to be present in displays of *grahami* group members for a display to contribute to the unit duration and standardized peak amplitude data sets. The most conspicuous difference between Type A and B displays in *A. grahami* and *A. garmani* is the very brief duration of Unit 2 relative to Unit 4 in Type B displays (Jenssen 1981:fig.1 and table 1). We define this difference as the Unit 2:4 ratio, which readily distinguishes the two display types in these taxa.

Measurement of Display Action Patterns

Bobbing displays were copied digitally from video recordings and imported for measurement into Macintosh GraphClick (v3, Arizona Software, Switzerland). Vertical (y-axis) motion of the head was tracked in video frames by placing a cursor over a subject's eye and clicking the mouse. The cursor coordinates were exported to Microsoft Excel (v14.7, Microsoft Corporation, Redmond, Washington) where they were plotted as Display Action Pattern (DAP) graphs and were subsequently measured.

Given that subjects were recorded in the lab and field at varying focal distances, we standardized (normalized) all bobbing displays to a unitless head amplitude scale of 0 to 1. This standardization was achieved by first subtracting the smallest (y-axis) value from each value in a display, followed by dividing each transformed value by the display's largest value. For display unit analyses, we assigned odd numbers (e.g., 1, 3, 5) to units in which the head was moving vertically, and even numbers to units in which head motion was paused. Display unit durations (resolution = 0.033 s) then were measured for all units and standardized bob peak amplitudes were measured in odd-numbered units.

We present descriptive statistics (median, range, and coefficient of variation [CV]) for unit durations and standardized peak amplitudes of all taxa in this study as Supplemental Tables S2–S20, available online. For the coefficient of variation, we followed a convention in which a behavior pattern with a CV <35% is considered stereotyped (Barlow 1977). Video clips of most display types analyzed in this study are provided as Supplemental Materials, available online, together with a list of video captions.

Fourier Transformation of Bobbing Displays

Their oscillatory nature makes bobbing displays analogous to a cluster of trigonometric functions. In MATLAB (vR2016b, MathWorks®, Natick, Massachusetts) we used the Fast Fourier Transform to compute the Discrete Fourier Transform (DFT) for each display. Fourier transformation subdivided each display into a series of sinusoidal waves with differing frequencies and amplitudes. Summing these sine functions recreates the original display. Whereas large amplitudes in the DFT of a display tend to occur at low frequency, low amplitudes tend to occur at high frequency and usually represent spurious noise in the signal. We reduced our amplitude threshold to 75% of the mean amplitude to exclude much of this noise. By comparing the reverse Fourier transform of the simplified signal to the original, we confirmed that filtering the transformed displays in this manner had not removed their distinctive features.

The variable anticipated to best capture taxon-specific attributes of bobbing displays was the frequency corresponding to the maximum amplitude: the Principal Frequency (Table 1). This variable describes the most pronounced trigonometric function underlying display structure. To further describe transforms of the displays, the frequency domain was partitioned into low (0–5 Hz), medium (5–10 Hz), and high (10–15 Hz) frequency ranges. Within each range we extracted four variables: peak frequency, the sum of the range amplitudes, the proportion of this sum relative to the total sum of range amplitudes, and the range's mean amplitude (Table 1). The four variables measured within each of three frequency ranges, plus the Principal Frequency, provided 13 variables to describe our Fourier transformed bobbing displays.

Comparative Analysis of Display Structure

For the three of our seven study species that possess recognized subspecies or otherwise distinctive populations (*A. conspersus, A. grahami,* and *A. lineatopus*), we used nested ANOVAs with a purely heuristic goal: to determine the relative proportions of variation in display structure contributed by within-subject, among-subject, and among-population variance (Lovern et al. 1999; Macedonia and Clark 2003; Macedonia et al. 2015b). We were particularly interested to assess which attributes of display structure differed most among subspecies and populations of a species, and whether those features were similar for the three species. For nested ANOVA calculations of variance proportions, we used a purposed Excel spreadsheet available in The Handbook of Biological Statistics (McDonald 2014).

Data exploration in SPSS (v21.0, IBM Inc., Armonk, New York) showed that many of our variables either were nonnormally distributed, significantly correlated, or both.

We therefore used principal components analysis (PCA) to obtain a smaller number of uncorrelated, normally distributed variables (i.e., principal components). We rotated the components (using Varimax rotation) to increase their interpretability relative to our original variables, and we retained those components that exceeded Jolliffe's (2002) criterion. Jolliffe (2002) found through simulation studies that a cut-off eigenvalue of 0.7, as opposed to the commonly used eigenvalue value of 1.0, increases retention of components that are likely explain important variation relative to the original variables. Principal component scores then were entered into a canonical discriminant function analysis (DFA) to determine how accurately displays could be correctly assigned to the taxon that produced them. In each analysis a cross-validated (leave-one-out) DFA also was performed, in which the display being classified was excluded from generation of the discriminant functions. In all discriminant analyses the smallest group size (i.e., taxon sample size) was larger than the number of predictor variables (i.e., principal components). For each taxon in each comparison, we used a Chi-squared goodness-of-fit test to assess whether the observed versus expected classification outcomes differed significantly from chance. Chi-squared goodness-of-fit tests were performed in VassarStats (Lowry 2020)—a statistical calculation website maintained by Vassar College that we have used previously for simple, repetitive tests (i.e., Macedonia et al. 2015b, 2016, 2019; Clark et al. 2019).

To reduce effects of autocorrelation arising from use of multiple samples per subject in a DFA (Mundry and Sommer 2007), we performed permuted discriminant function analyses (pDFA) in Program R (v3.3.2; R Core Team 2016) using a function provided by R. Mundry (2015) based on lda in the R package MASS. The control factor (subject) was nested within the test factor (taxon) in our pDFAs. We set each pDFA to randomly select two displays from each subject to generate the discriminant functions that classified the displays to taxon. The selection process was iterated 100 times and the subsequent classifications were averaged. Each pDFA then permuted the displays among taxa 1000 times to determine whether average classification success differed significantly from the random assignment of displays (i.e., the null hypothesis). As in a standard DFA, pDFA runs a cross-validated analysis in which half of the displays are used to create the discriminant functions that classify the remaining displays. We present results only from the cross-validated pDFAs because, as in all cases, results of the original pDFAs were identical to those of our standard DFAs.

DFA Classification Success: Testing at Different Levels

We compared DFA classification success at inter- and intraspecific levels using unit-based variables, DFT-based variables, and the combination of the two approaches. The one exception to this protocol was the analysis of *A. lineatopus* displays, for which we used only DFT variables on account of the ambiguity of partitioning displays into units for our subspecies. In each analysis we present detailed results for the most successful of the three approaches and summarize the outcomes of the two less successful methods.

To avoid biasing our discriminant analyses of subspecies and populations in favor of taxa for which we had larger samples, we sought to choose 4 displays from 4 subjects of each taxon, totaling 16 displays per taxon. In a few cases, where the sample of subjects was small and a subject possessed <4 (but ≥ 2) displays, we achieved a total of 16 displays by adding displays from one or two subjects already included in the analysis (Supplemental Table S21, available online). We also present a *grahami* group among-species analysis, which included 16 displays from each of 3 *A. grahami* populations (48 total displays), 16 displays from each of the 3 *A. conspersus* populations (48 total displays), and 48 displays from the monotypic *A. opalinus* (Supplemental Table S21).

Following each discriminant analysis, we used Kruskal–Wallis ANOVAs to test the null hypothesis that the discriminant scores from the three taxa being compared (either species or subspecies–populations) were drawn from the same distribution. When results were significant, we carried out pairwise tests using the same Kruskal–Wallis test, in which calculations are identical to the Mann–Whitney *U*-Test. For our Kruskal–Wallis ANOVAs, we used a purposed spreadsheet from The Handbook of Biological Statistics (McDonald 2014) that provides exact *P*-values up to 30 decimal places. As we conducted multiple Kruskal–Wallis ANOVAs involving the same sets of discriminant scores (i.e., one three-way test plus three pairwise tests for each of two discriminant functions = eight tests), we used the sequential Holm–Bonferroni method for *P*-value correction to reduce the probability of Type 1 error (spreadsheet from Gaetano 2013).

Finally, DFA results in Macedonia et al. (2019) suggested that classification success of DFT-characterized Galápagos Lava Lizard displays was more successful for species with relatively simple displays than for species with structurally more complex displays. In the present study we tested the generality of this finding using four display types of *A. reconditus* that differ in structural complexity: the simpler Type B_2 and B_4 displays, and the compound Type B_2+A and B_4+A displays (Figs. 13, 14). We predicted that the simpler display types would more often correctly be classified in a DFA than would be the more complex display types. ?1

Results

Bobbing Display Structure in the *Anolis grahami* Group

Anolis conspersus.—Among members of the *grahami* group, *A. conspersus* is unique in possessing two types of stereotyped bobbing displays (Type A and B) that differ vastly in structure (Macedonia and Clark 2001). In the Type A display, the initial bob (Unit 1) exhibits a spike + plateau shape that closely resembles bobs in the displays of *A. g. grahami* from Kingston and Mandeville (Fig. 3A; Supplemental Tables S2, S4, S6). However, all subsequent bobs in the display are spike-shaped like those of *A. g. grahami* from western Jamaica (Negril; Jenssen 1981) and *A. g. aquarum* from eastern Jamaica (see below). Durations of most units were stereotyped among subjects, whereas the final two pauses in the display exhibited low stereotypy (Supplemental Tables S2, S4, S6). Total display duration also was stereotyped among subjects, as were all five standardized peak amplitudes. Type A displays were produced both individually and in volleys (color morphs combined; $n = 37$ volleys, median = 3 displays/volley, range = 2–6 displays/

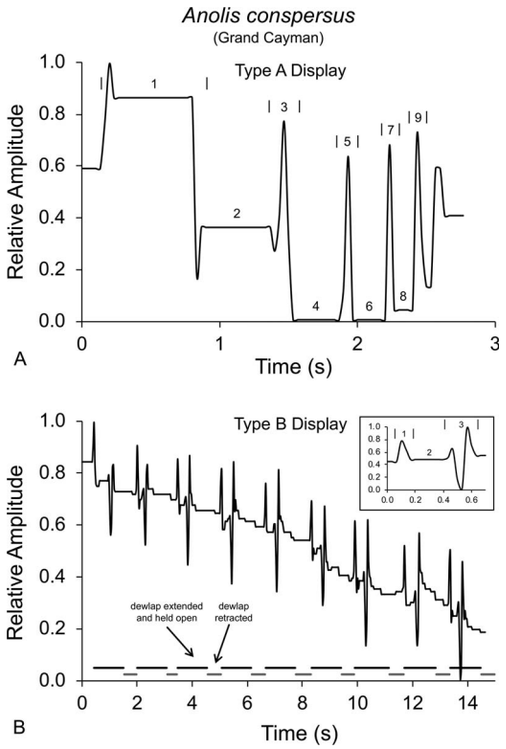

FIG. 3.—*Anolis conspersus* (Grand Cayman) amplitude-standardized bobbing displays. (A) *A. conspersus* Type A display. Numbers above display show unit numbers; brackets framing odd numbers demarcate bob unit durations measured for the first nine units. Standardized peak amplitudes measured for bobs (Units 1, 3, 5, 7, and 9). Dewlap pulses not shown but occur immediately following the bobbing display as they do in *A. grahami* (see Figs. 4–6). Descriptive statistics for measurements of unit durations and standardized peak amplitudes presented in Supplemental Tables S2, S4, and S6. (B) *A. conspersus* Type B display volley of nine consecutive displays (inset shows a single display). Descriptive statistics for measurements of unit durations and standardized peak amplitudes presented in Supplemental Tables S3, S5, and S7. Dewlap pulses shown at bottom of graph: thick black lines indicate the duration of time in which the dewlap is extended and held open, and the thick gray lines indicate the duration of time over which the dewlap is retracted.

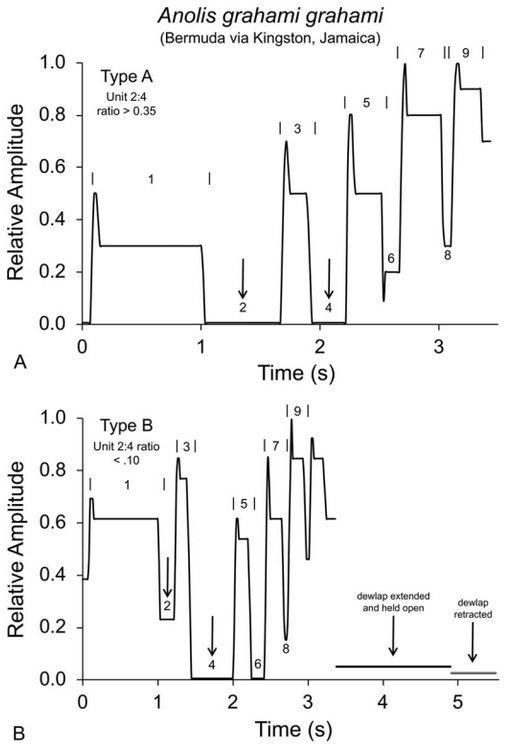

FIG. 4.—*Anolis grahami grahami* (Bermuda via Kingston, Jamaica) amplitude-standardized bobbing displays. (A) Type A and (B) Type B displays. Unit 2:4 duration ratios distinguishing the two display types were determined from our data and are consistent with those of Jenssen (1981). Several cycles of dewlap extension and retraction are common following both types of bobbing displays. Descriptive statistics for measurements of unit durations and standardized peak amplitudes presented in Supplemental Tables S8 and S9. Legend as in Fig. 3.

volley). Typically, the dewlap extends and retracts once immediately before bobbing begins (termed a "prior-pulse"; Jenssen 1979a). The dewlap then is pulsed one or more times at the end of each display, as occurs in other *grahami* group species (Jenssen 1977a:fig. 7).

Anolis conspersus Type B displays (Fig. 3B; Supplemental Tables S3, S5, S7) were performed in volleys that typically contained numerous displays (color morphs combined; n = 34 volleys, median = 8 displays/volley, range = 3–15 displays/volley). The brief and rapidly produced Type B display consists of three units, beginning with spike-shaped bob (Unit 1) that is followed by a brief pause (Unit 2) and a spike–dip–spike head motion (Unit 3). Durations of all display units and standardized peak amplitudes were stereotyped, with the singular exception of Unit 2 duration in the blue morph (Supplemental Table S7). Although the dewlap is pulsed once between each Type B display in a volley, dewlap pulsing and bobbing are not tightly synchronized, with varying degrees of overlap occurring between them as a volley proceeds (Fig. 3B; Macedonia and Stamps 1994:fig. 4). Last, *A. conspersus* also engaged in step-bobbing (see *A. grahami* below for description).

Anolis grahami.—Bobbing displays in each of our three study populations of *A. grahami* are structurally distinct. First, displays of *A. grahami grahami* on Bermuda do not differ from those of their founder population in Kingston, Jamaica (Macedonia and Clark 2003). Each bob in the display is plateau-shaped and is prefixed with a spike (Fig. 4), as has been illustrated for this subspecies from Mandeville, Jamaica (Jenssen 1977b:fig. 3). The spike arises from the recoil that follows rapid vertical acceleration of the head and a sudden stop at the apex of the head movement. Similar to Jenssen's (1981) findings for *A. g. grahami* from Mandeville and Kingston, bobbing displays from our Bermudian population were easily distinguished into Type A and B displays. We found that Unit 2:4 duration ratios either were <0.1 (Type A) or were greater than ≈ 3.5 (Type B). In contrast, comparable data from our *A. g. grahami* population on the north-central coast of Jamaica (Discovery Bay; Fig. 5), as well as from *A. grahami aquarum* in northeastern Jamaica (Dragon Bay; Fig. 6), exhibited continuous distributions of Unit 2:4 ratios from the lowest to highest values. We therefore provide descriptive statistics separately for Type A and B displays in our Bermuda *A. g. grahami* population (Supplemental Tables S8, S9), but we do not make this distinction in our Discovery Bay *A. g. grahami* population

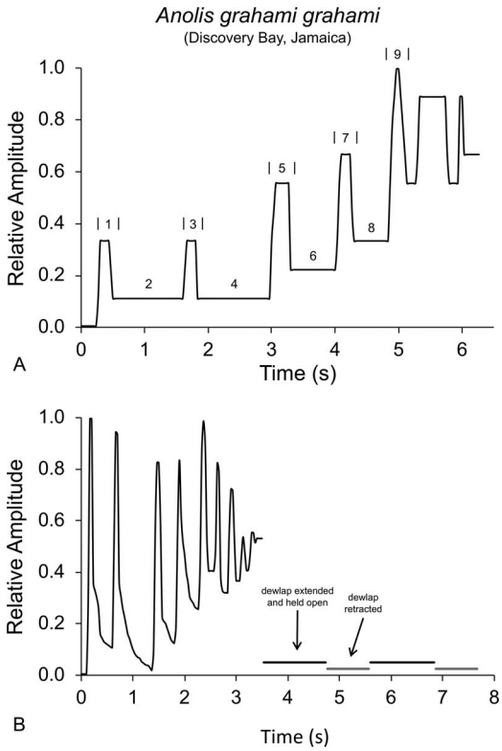

FIG. 5.—*Anolis grahami grahami* (Discovery Bay, Jamaica) amplitude-standardized bobbing displays. In contrast to *A. g. grahami* from Bermuda (via Kingston, Jamaica), Unit 2:4 duration ratios determined from our data did not support dividing displays into types. Descriptive statistics for measurements of unit durations and standardized peak amplitudes presented in Supplemental Table S10. Legend as in Figs. 3, 4.

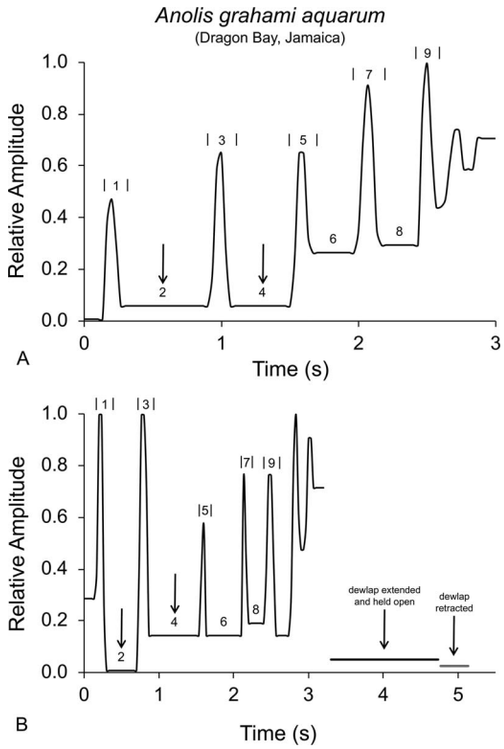

FIG. 6.—*Anolis grahami aquarum* (Dragon Bay, Jamaica) amplitude-standardized displays. As for *A. grahami grahami* (Discovery Bay, Jamaica), Unit 2:4 duration ratios determined from our data did not support dividing displays into types. Descriptive statistics for measurements of unit durations and standardized peak amplitudes presented in Supplemental Table S11. Legend as in Figs. 3, 4.

(Supplemental Table S10) or in *A. g. aquarum* (Supplemental Table S11).

In Type A displays of our Bermuda *A. g. grahami* population, durations of all nine units except the final pause, total display duration, and all five standardized peak amplitudes were stereotyped (i.e., CV <35%; Supplemental Table S8). In Type B displays from this population, seven of the nine unit durations were stereotyped, but pause Units 2 and 6 were highly variable among subjects (Supplemental Table S9). By comparison, in our Discovery Bay *A. g. grahami* population (Supplemental Table S10) and in *A. g. aquarum* (Supplemental Table S11), all durations and standardized peak heights were stereotyped except for the peak height of Unit 1.

The dewlap display is performed in the same manner in all three of our *A. grahami* study populations. Like *A. conspersus* Type A displays, *A. grahami* may produce a prior-pulse before bobbing commences, and the dewlap typically is pulsed several times at or near the end of the bobbing display (Jenssen 1979a; Macedonia and Stamps 1994:fig. 1). Finally, like *A. conspersus* and several other *grahami* series taxa (see below), we observed *A. grahami* (Fig. 7) step-bobbing, a type of display described by Jenssen (1979a) for *A. opalinus*. Although step-bobbing can exhibit a relatively uniform pattern of motion both temporally and in degree of head amplitude change (Fig. 7), it possesses comparatively low stereotypy in comparison with taxon-specific bobbing displays (Jenssen 1979a).

Anolis garmani.—Bobbing displays in *A. garmani* (Fig. 8; Supplemental Tables S12, S13) are structurally similar to those of *A. grahami aquarum*. The cadence of *A. garmani* displays is slower, however, perhaps as a result of the much larger body size of this species (Supplemental Table S1). Like the Jamaican (Kingston and Mandeville) and Bermudian populations of *A. g. grahami*, *A. garmani* possesses Type A and Type B displays with nonoverlapping Unit 2:4 ratios (Fig. 8). In our very small sample (one Type A display each from three subjects; Supplemental Tables S12, S13), this display type had a Unit 2:4 ratio of 2.0. In contrast, Unit 2:4 ratios in the two Type B displays that we recorded were

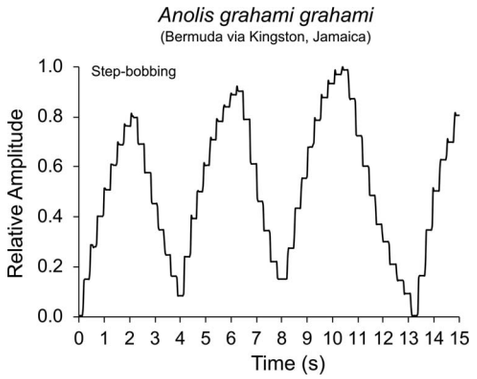

FIG. 7.—*Anolis grahami grahami* (Bermuda) amplitude-standardized step-bob display.

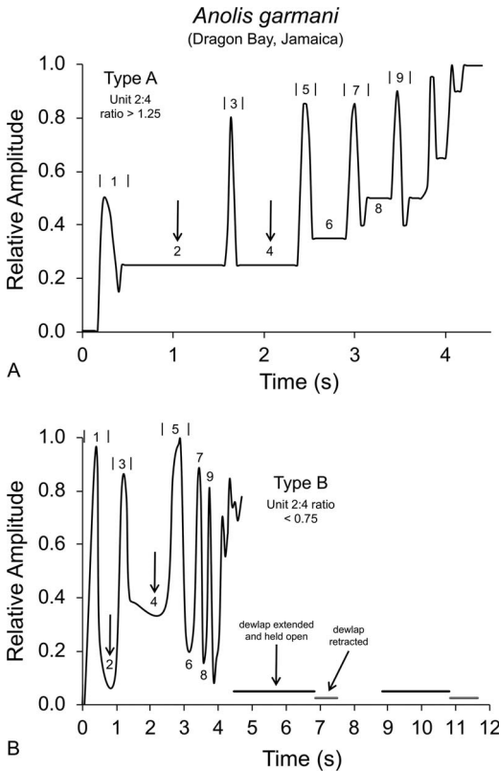

FIG. 8.—*Anolis garmani* amplitude-standardized bobbing displays. (A) Type A display. (B) Type B display. Unit 2:4 duration ratios distinguishing the two display types determined from our data and are consistent with those of Jenssen (1981). Descriptive statistics for measurements of unit durations and standardized peak amplitudes presented in Supplemental Tables S12 and S13. Legend as in Figs. 3, 4.

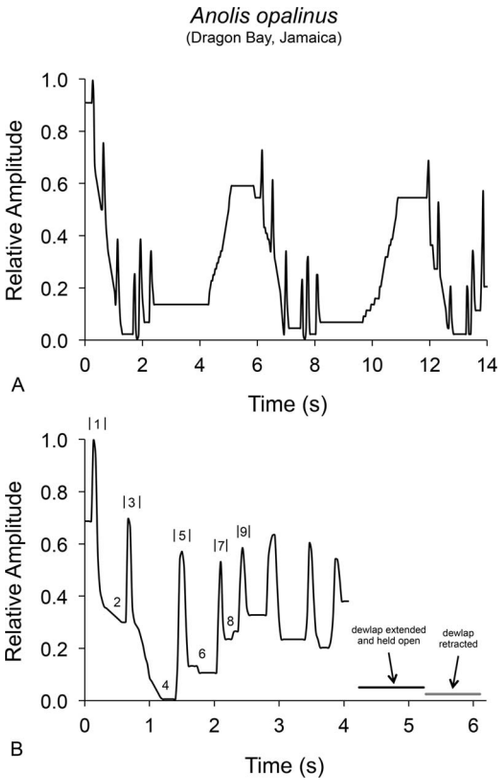

FIG. 9.—*Anolis opalinus* amplitude-standardized bobbing displays. (A) Volley of three bobbing displays containing six bobs each. (B) Single display containing eight bobs and a single dewlap pulse shown. Several cycles of dewlap extension and retraction were common following the final bobbing display in a volley as well as displays not performed in volleys. Descriptive statistics for measurements of unit durations and standardized peak amplitudes are shown in Supplemental Table S14. Legend as in Figs. 3, 4.

below 1.0 (0.437 and 0.742). These values are consistent with Unit 2:4 ratios that we calculated from Jenssen's (1981) unit-based data for three male *A. garmani* from Mandeville (Type A = 1.270, Type B = 0.503).

Anolis opalinus.—Jenssen (1979b) detailed *A. opalinus* bobbing display structure from 51 males at locations throughout Jamaica, excluding the northeastern part of the island where we collected our subjects (Dragon Bay, Portland Parish). In addition, Jenssen (1979a) described numerous aggressive postures and display movements that accompanied bobbing displays, most of which also have been analyzed for *A. g. grahami* from Discovery Bay (Macedonia and Stamps 1994). In contrast to other *grahami* group species, Jenssen (1979b) found that *A. opalinus* bobbing displays exhibited comparatively low stereotypy, wherein displays contained between 4 and 11 bobs and were followed by 0 to 8 dewlap pulses. By comparison, we recorded 87 bobbing displays from 7 males that contained from 5 to 8 bobs (median = 7.0) with 0 to 7 dewlap pulses (median = 2.0) following the display (Fig. 9). Our data therefore fall within Jenssen's (1979b) more extensive data set. We used a smaller data set of 54 bobbing displays from our 7 males for which unit durations and standardized peak amplitudes could be accurately calculated (Supplemental Table S14). Excluding the final two pause units, display unit durations were stereotyped, as was total display duration and four of the five standardized peak amplitudes (Supplemental Table S14).

Bobbing Display Structure in the *Anolis lineatopus* Group

Anolis lineatopus.—With four subspecies, *Anolis lineatopus* is the most taxonomically diverse species in the *grahami* series radiation. Nevertheless, bobbing displays from only one of the four subspecies, *A. l. neckeri*, have been described to date. Jenssen (1977b:fig. 3) illustrated the *A. l. neckeri* signature display as being very brief (≈ 1 s), with three bobs that were produced in a sine-wave pattern. The author noted that the dewlap extension and retraction did not occur during bobbing but infrequently followed the display. Jenssen (1977b) also noted that about one-third of the 93 displays he recorded from 4 males had been produced in pairs that were separated by a pause (≈ 0.3 s).

Although we were unable to observe *A. l. neckeri,* we recorded displays from the three remaining *A. lineatopus* subspecies: *A. l. lineatopus, A. l. ahenobarbus,* and *A. l. merope*. In contrast to Jenssen's (1977b) description of *A. l. neckeri* displays, we found displays from our *A. lineatopus* subspecies to be highly variable in duration and in structure. Displays often appeared to exhibit little organizational pattern and lasted from <1 s to >7 s (Fig. 10). Although lengthy *A. lineatopus* bobbing displays appeared to be volleys (Fig. 10B), the distinction between individual

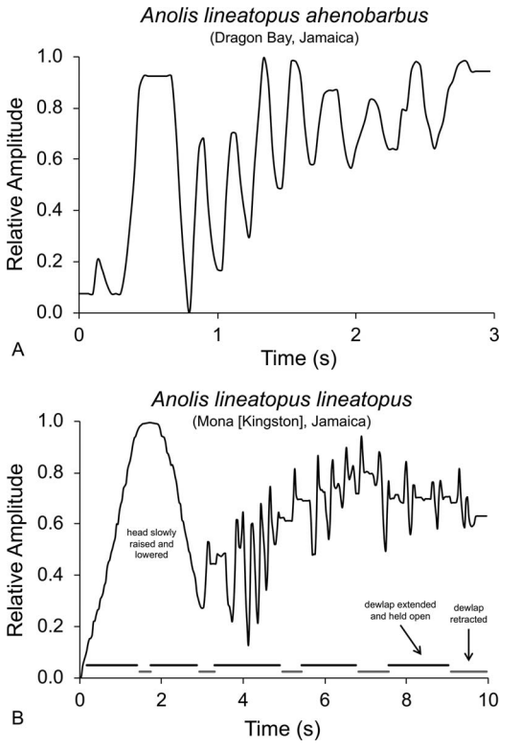

FIG. 10.—Amplitude-standardized bobbing displays in (A) *Anolis lineatopus ahenobarbus* and (B) *A. lineatopus lineatopus*. In Panel B, the slow head raising and lowering just prior to the bobbing display was present only in the first display in a volley. Illustration of dewlap pulsing as in Fig. 3.

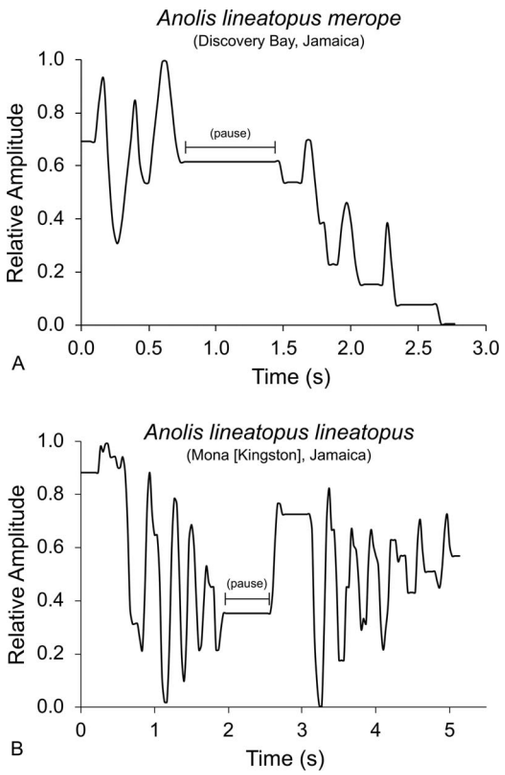

FIG. 11.—Amplitude-standardized bobbing displays in (A) *Anolis lineatopus merope* and (B) *A. lineatopus lineatopus*. Both displays feature the presence of a mid-display pause.

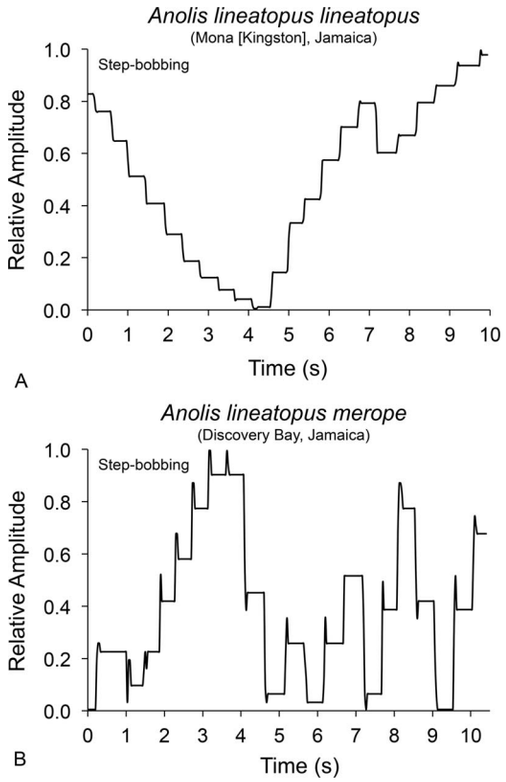

FIG. 12.—Amplitude-standardized step-bobbing displays in (A) *Anolis lineatopus lineatopus* and (B) *A. lineatopus merope*.

displays and volleys was rarely clear, and we found display structure to be too variable to consistently assign displays to a type. Dewlapping occurred during bobbing (cf., Jenssen 1977b), but dewlap extension and retraction had no apparent temporal relationship to bobbing (Fig. 10B). Although we observed the three-bob sinusoidal display pattern (Fig. 11A) and the paired display pattern (Fig. 11A, B) that Jenssen (1977b) described for *A. l. neckeri*, we found that pauses exhibited a continuous distribution (≈ 0.2–1.0 s) and could occur at any location or in multiple locations within a display or volley. The very low structural stereotypy of bobbing displays in our *A. lineatopus* subspecies led us to abandon the prospect of measuring unit-based variables and calculating CVs. Nevertheless, the continuously varying structure of these displays made them ideal for the DFT approach to bobbing display analysis. Last, as in many of our other *grahami* series taxa, we observed step-bobbing in *A. lineatopus* (Fig. 12).

***Anolis reconditus*.**—*Anolis reconditus* possesses the most diverse bobbing display repertoire of any species in the *grahami* series radiation. We documented seven types of bobbing displays that we place into two categories: simple displays (Types A, B_1, B_2, B_3, and B_4) and compound displays (Types B_2+A and B_4+A). We illustrate each display type schematically to provide examples of variations within display types and to show how we made our unit-based measurements (Fig. 13). Displays usually were performed in volleys that contained multiple display types (Fig 14; Supplemental Tables S15–S18). We measured standardized peak amplitudes only for displays that contained Type A units, because the morphology of peak-like and plateau-like

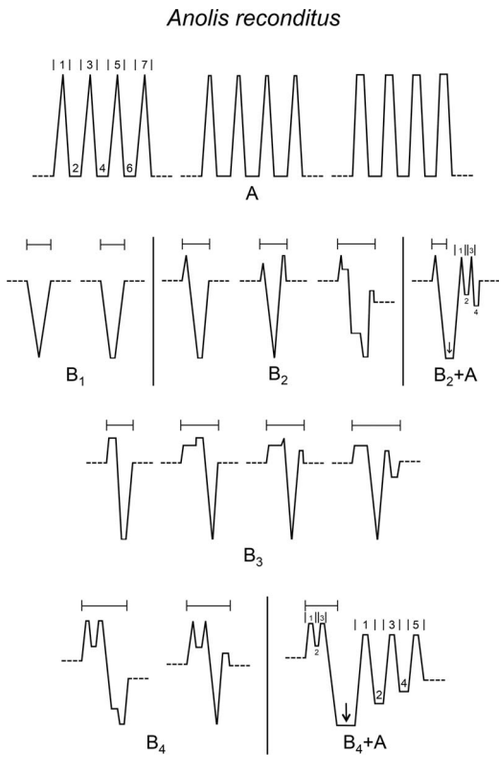

FIG. 13.—Schematic representation of *Anolis reconditus* bobbing display diversity divided into simple and compound displays. Horizontal bars with end caps above each display indicate the portion of the display measured in addition to number-demarcated units. Simple Displays—Row 1: Type A displays comprise repetitions of peaked or flat-topped spike-like units. Durations of the first seven units were measured in Type A displays, as were standardized peak amplitudes in Units 1, 3, 5, and 7 (Supplemental Table S15). Row 2: Type B_1 displays comprise a simple lowering and raising of the head. Type B_2 displays add a quick, sharp-peaked upswing just prior to lowering and raising the head. Row 3: Type B_3 displays exhibit a head upswing with a plateaued square-wave shape rather than a sharp peak. Row 4: Type B_4 displays begin with a rapid double-bob, in which the head is not lowered completely until after the second bob. Compound Displays—Row 2 (end): Type B_2+A displays concatenate Type B_2 and Type A display types. The arrow between the Type B_2 and Type A components points to a pause whose duration was measured. Row 4 (end): Type B_4+A displays concatenate Type B_4 and Type A display types. Measurements as for Type B_2+A displays.

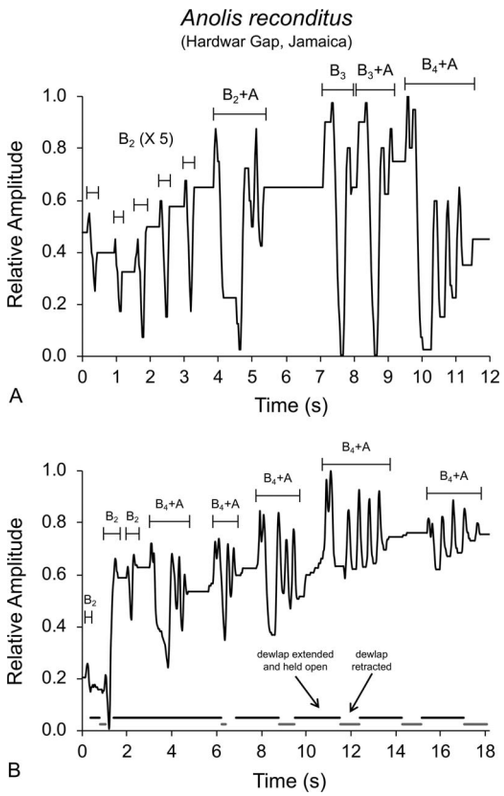

FIG. 14.—Two examples of *Anolis reconditus* amplitude-standardized display volleys. Horizontal bars with end caps indicate the start and end of each display. Descriptive statistics for measurements of display durations, unit durations and standardized peak amplitudes are presented in Supplemental Tables S15–S18. Legend for dewlap extension and retraction as in Fig. 3.

structures prior to the head dip in display Types B_2 and B_3 (Fig. 13) lacked sufficient uniformity to measure with confidence. The *A. reconditus* Type B_4+A display contained from two to four Type A units, and we required this display to contain at least three Type A units to be included in our calculations of display duration (Supplemental Table S18). Similar to our *A. lineatopus* subspecies, extension and retraction of the dewlap in *A. reconditus* displays appeared to be independent of bobbing. Finally, as in most of our study species we observed step-bobbing in *A. reconditus* (Fig. 15).

Bobbing Display Structure in *Anolis valencienni*

Anolis valencienni.—Bobbing displays in *A. valencienni* are a subset of those occurring in *A. reconditus:* Types A, B_1, B_2, and B_3 (Fig. 13; Supplemental Tables S19, S20). In our only recorded occurrence of an *A. valencienni* Type A display (Fig. 16A), it is unclear whether the Type A display is independent of the Type B_1 display that precedes it or whether it represents a compound display. In contrast to *A. reconditus*, dewlapping in *A. valencienni* exhibited almost no overlap with bobbing during displays (Fig. 16B).

Within-Subject, Among-Subject, and Among-Population Display Variance

Anolis conspersus.—For Type A displays, a nested ANOVA revealed that most of the variance in bobbing display unit durations was within subjects (median = 53.3%),

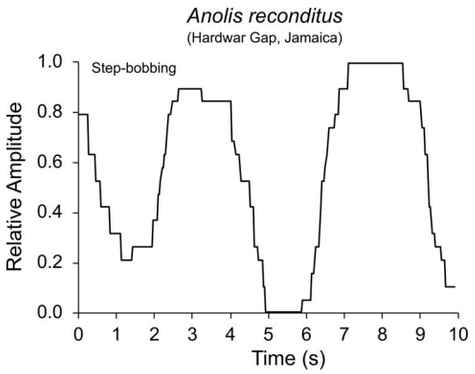

FIG. 15.—Example of an amplitude-standardized *Anolis reconditus* step-bobbing display.

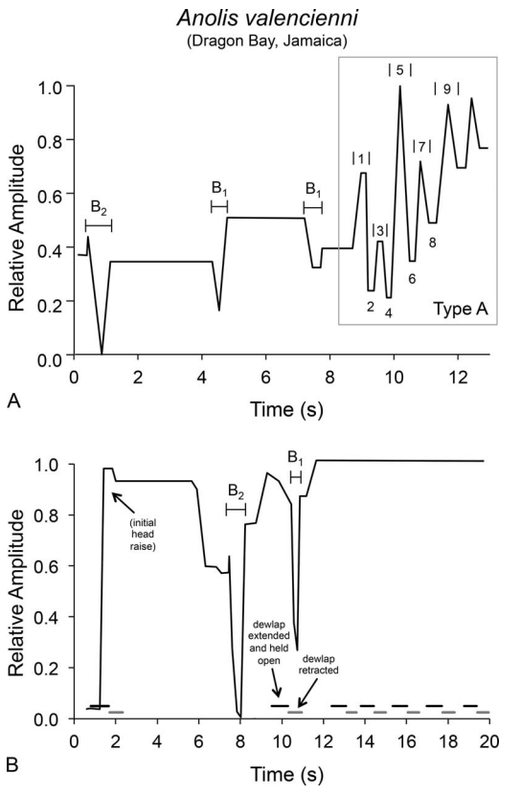

FIG. 16.—Two examples of *Anolis valencienni* amplitude-standardized display volleys. (A) Volley containing Type a B_2 display, two Type B_1 displays, and a Type A display (enclosed by the gray line and indicating the units whose durations were measured). Horizontal bars with end caps indicate the start and end of each Type B display variant. Descriptive statistics for unit durations and standardized peak amplitudes presented in Supplemental Tables S18 and S19. Legend for dewlap extension and retraction as in Fig. 3.

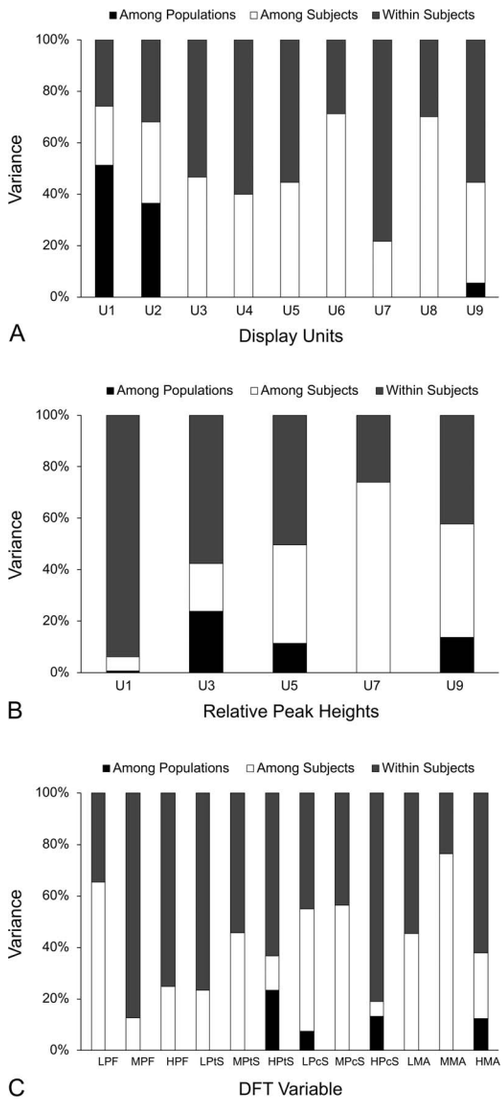

FIG. 17.—Stacked bar charts showing the sources and proportions of bobbing display variance in *Anolis conspersus* Type A displays, as determined in a nested ANOVA. For each measure the three sources of variance add to 100%. Populations include the green morph (*A. c. conspersus*), the brown morph (*A. c. lewisi*), and a taxonomically unrecognized blue morph. (A) Proportions of variance attributable to display unit durations in the first 9 units of Type A displays. (B) Proportions of variance attributable to standardized peak amplitudes in first 5 bob units of Type A displays. (C) Proportions of variance attributable to 12 Discrete Fourier Transform (DFT) variables measured for Type A displays. Abbreviations: LPF = Low Peak Frequency, MPF = Medium Peak Frequency, HPF = High Peak Frequency, LPtS = Low (frequency) Partial Sum, MPtS = Medium (frequency) Partial Sum, HPtS = High (frequency) Partial Sum, LPcS = Low Percentage of Sum, MPcS = Medium Percentage of Sum, HPcS = High Percentage of Sum, LMA = Low Mean Amplitude, MMA = Medium Mean Amplitude, HMA = High Mean Amplitude. Low = 0–5 Hz, Medium = 5–10 Hz, High = 10–15 Hz. For additional details, see Table 1.

followed by variation among subjects (median = 40.1%; Fig. 17A). Only three of the nine display units exhibited measurable among-population (color morph) variation (Fig. 17A). Here, Unit 1 was briefer and Unit 2 was lengthier in the brown morph (*A. c. lewisi*) than in the green and blue morphs (Supplemental Tables S2, S4, and S6). A nested ANOVA performed on Type A display peak amplitudes revealed a pattern similar to that of unit durations: within-subject variance was greatest (median = 50.3%) and was again followed by among-subject variance (median = 38.3%; Fig. 17B). Among-population variance in standardized peak amplitudes was minor (median = 11.4%), with Unit 3 exhibiting the greatest proportion of variability (23.8%; Fig. 17B).

Finally, we conducted a nested ANOVA on 12 DFT variables for Type A displays. We excluded Principal Frequency from nested ANOVAs of DFT variables because it was highly redundant with Low Peak Frequency. As in unit-based measurements, the largest proportion of variation was observed within subjects (median = 58.5%), followed by variation among subjects (median = 35.5%; Fig. 17C). Among-population variance was low (median = 0.0%), with only four variables exhibiting nonzero variance (Fig. 17C).

Type B displays showed a somewhat different pattern of unit duration variance than Type A displays. Although within-subject variance was still the greatest source of variation in Type B displays (median = 42.5%), among-population variance was the second largest source of variation (median = 35.4%), followed by among-subject variance (median = 22.7%; Fig. 18A). The three standardized peak amplitudes also differed substantially in their

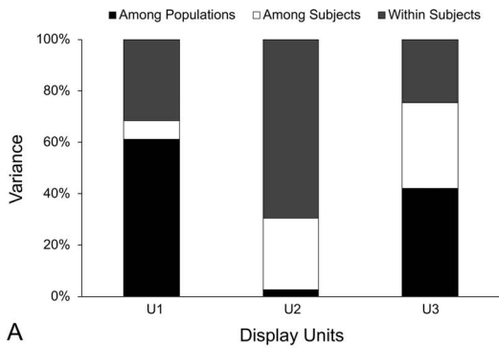

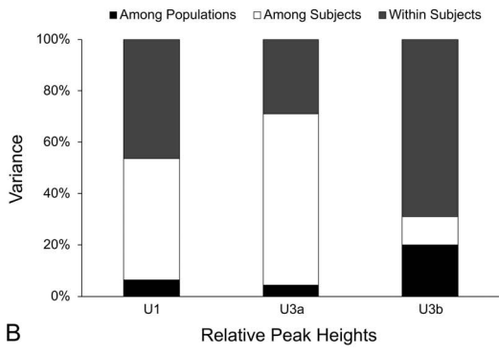

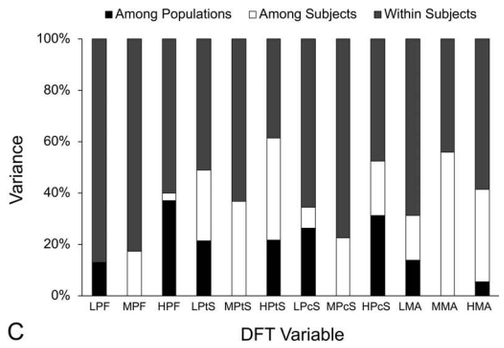

FIG. 18.—Stacked bar charts showing the sources and proportions of bobbing display variance in *Anolis conspersus* Type B displays, as determined by a nested ANOVA. (A) Proportions of variance attributable to display unit durations in Type B displays. (B) Proportions of variance attributable to standardized peak amplitudes in Type B displays. (C) Proportions of variance attributable to 12 Discrete Fourier Transform (DFT) variables measured for Type B displays. Legend as in Fig. 17.

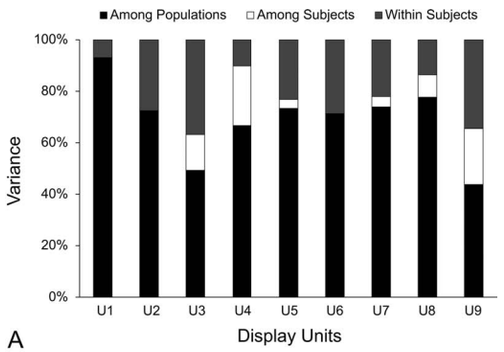

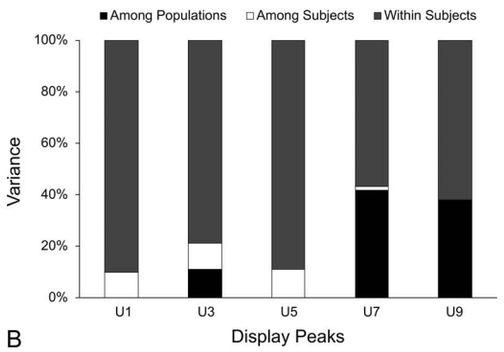

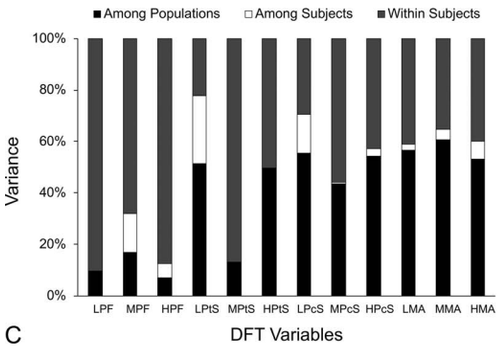

FIG. 19.—Stacked bar charts showing the sources and proportions of bobbing display variance in *Anolis grahami* displays, as determined by a nested ANOVA. Populations include *A. g. grahami* (Kingston and Bermuda), *A. g. grahami* (Discovery Bay, Jamaica), and *A. g. aquarum* (Dragon Bay, Jamaica). (A) Proportions of variance attributable to display unit durations in the first 9 units of displays. (B) Proportions of variance attributable to unit durations and standardized peak amplitudes in first 5 bob units of displays. (C) Proportions of variance attributable to 12 Discrete Fourier Transform (DFT) variables measured for displays. Display type is Type A for the Kingston–Bermuda population and is undefined for the Discovery Bay and Dragon Bay populations (see text). Legend as in Fig. 17.

distribution of variance (Fig. 18B). Our DFT variables showed within-subject variance to be the largest source of variation (median = 61.5%), followed by among-subject (median = 21.9%) and among-population variance (median = 13.5%). In contrast to Type A displays, among-population variation was present in the majority of DFT measures (8 of 12 variables) for Type B displays (Fig. 18C).

Anolis grahami.—In *A. grahami,* among-population variance accounted for most of the variation in display unit durations (median of 9 units = 72.4%), with most of the remaining variation being attributable to within-subject variation (median = 23.1%; Fig. 19A). Like A. *conspersus* Type A displays, among-population variance in *A. grahami* accounted for most of the duration variation in Unit 1 (93.0%) and Unit 2 (73.3%). Unlike *A. conspersus,* however, all nine *A. grahami* display units exhibited considerable among-population variance, which accounted for the majority of variation in most units. Close examination of the three units in which there was no among-subject variation (Units 1, 2, and 6) explained why among-population variation in *A. grahami* unit durations was so large. Whereas the Kingston–Bermuda population exhibited lengthy Unit 1 durations (median = 1.13 s) and brief Unit 2 durations (median = 0.30 s; Supplemental Table S8), the Discovery Bay population showed the opposite pattern of brief Unit 1 durations (median = 0.33 s) and lengthy Unit 2 durations (median = 1.00 s; Supplemental Table S10). The subspecies *A. g.*

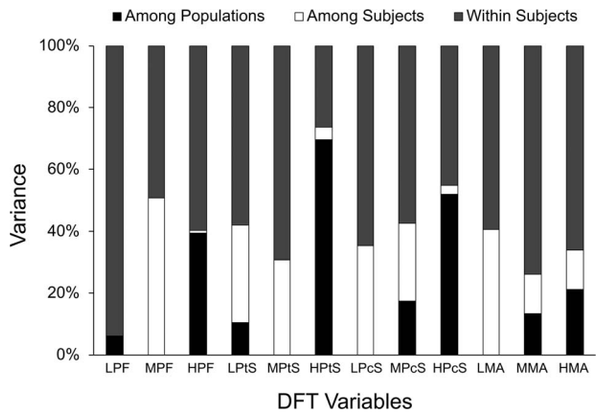

FIG. 20.—Stacked bar charts showing the sources and proportions of variance attributable to 12 Discrete Fourier Transform (DFT) variables measured for bobbing display variance in *Anolis lineatopus* displays, as determined by a nested ANOVA. Populations include *A. l. lineatopus* (Kingston, Jamaica), *A. l. ahenobarbus* (Dragon Bay, Jamaica), and *A. l. merope* (Discovery Bay, Jamaica).

aquarum (Dragon Bay) was most similar to Discovery Bay *A. g. grahami*, with very short Unit 1 durations (median = 0.17 s) and longer Unit 2 durations (median = 0.63 s; Supplemental Table S11).

Although within-subject variation accounted for most of the variance in standardized peak amplitudes (median = 78.8%), among-population variation in the standardized peak amplitudes of Unit 7 (41.7%) and Unit 9 (38.0%) suggested that bobbing peaks in these two units might distinguish *A. grahami* taxa (Fig. 19B). Whereas similarly large proportions of among-subject variance were present in *A. g. grahami* from Discovery Bay (median = 78.6%; Supplemental Table S10) and *A. g. aquarum* (median = 77.7%; Supplemental Table S11), among-subject variance in *A. g. grahami* (Kingston–Bermuda) was larger (93.6%; Supplemental Table S8). Thus, for measures that exhibited moderate to substantial among-population variation, the Discovery Bay population of *A. g. grahami* and the Dragon Bay population of *A. g. aquarum* were more similar to each other than either was to the Kingston–Bermuda population of *A. g. grahami*. We therefore predicted that *A. g. grahami* (Discovery Bay) and *A. g. aquarum* (Dragon Bay) should cluster closer together in discriminant function space than either should to the *A. g. grahami* population from Kingston–Bermuda (see below).

Last, for our DFT measures, among-population variance accounted for most of the variation (median = 50.7%), followed closely by within-subject variation (median = 46.4%; Fig. 19C). Similar to unit durations, among-subject variance in DFT measures contributed minimally to the total variation (median = 3.6%).

***Anolis lineatopus*.**—A nested ANOVA on DFT measures revealed that within-subject variance accounted for most of the variation in display structure (median = 59.5%; Fig. 20). Among-subject variance was substantially smaller (median = 19.1%), with the remainder of the variance being explained as among-population variation (median = 11.9%). For each variable type we found that high frequencies contained the largest percentages of among-population variation (Fig. 20).

DFA Classification Success of Unit-based and DFT-based Variables

With the exception of *A. lineatopus*, we conducted three separate PCA–DFA analyses on each trio of study taxa. In each case we provide detailed findings for the most successful analysis and summarize of the outcomes of the two less successful analyses.

***Grahami* group species.**—We carried out a PCA with our unit duration and standardized peak amplitude measures on 48 displays each from *A. conspersus*, *A. grahami*, and *A. opalinus* (Supplemental Table S21). For this species-level analysis we combined the three *A. conspersus* populations as well as the three *A. grahami* populations (16 displays from each population; Supplemental Table S21). The PCA retained five components with eigenvalues >0.7 (Jolliffe's criterion; Jolliffe 2002) that explained >85% of the variation in the data (Supplemental Table S22, available online). The first component (PC1) explained approximately 29% of the variation (Supplemental Table S22), and was most heavily weighted on bob unit durations and total display duration (Supplemental Table S23, available online). We entered the five components simultaneously into a DFA that produced two discriminant functions (Supplemental Table S24, available online). The first four components contributed strongly to these functions (see Supplemental Table S24 for *P*-values), with DF1 being most heavily weighted on PC3 (largely pause unit durations) and DF2 being most heavily weighted on PC1 (primarily bob unit durations). Together, the two discriminant functions assigned 134 of 144 displays (93.1%) to the correct species in the initial analysis and 133 displays (92.4%) in the cross-validation analysis (Table 2). Remarkably, 100% of the 48 *A. conspersus* displays were correctly classified to species in both analyses (Table 2). Chi-squared goodness-of-fit tests revealed that observed classification success was greater for each species than expected by chance in all cases, and most classification errors were due to *A. grahami* displays being incorrectly assigned to *A. opalinus* (Table 2). A scatterplot of the discriminant scores demonstrated that DF1 completely separated the displays of *A. conspersus* and *A. opalinus*, whereas DF2 was more effective at separating the displays of *A. grahami* from those of the other two species (Fig. 21). Kruskal–Wallis ANOVAs showed that discriminant scores differed among the three species on both axes, and differed between pairs of species in all Bonferroni-protected comparisons except one (Fig. 21, see insets; Supplemental Table S25, available online).

Lower performing DFAs: A DFA conducted with four principal components (PC) generated from our DFT variables produced two discriminant functions that were virtually as successful in assigning displays to species (i.e., one less correct assignment) as the unit duration and standardized peak amplitude variables. Correct classification was 92.4% (133 of 144 displays) in the original analysis and 91.7% (132 of 144 displays) in the cross-validation analysis. Last, a DFA performed on nine PCs created from the combination of unit-based and DFT-based variables produced two discriminant functions that correctly classified displays to species 86.1% (124 of 144 displays) in the original analysis and 83.3% (120 of 144 displays) in the cross-validation analysis.

TABLE 2.—Discriminant function analysis of 5 principal components derived from 15 unit duration/standardized peak amplitude variables that measured bobbing displays in our three *grahami* group species. We used Type A displays for *A. conspersus* (Grand Cayman: 16 displays each color morph) and *A. g. grahami* (Bermuda: 16 displays), as well as displays unclassified to type in *A. g. grahami* (Discovery Bay, Jamaica: 16 displays), *A. grahami aquarum* (Dragon Bay, Jamaica: 16 displays), and *A. opalinus* (Dragon Bay, Jamaica: 48 displays). Number (and percent) of correct display assignments in bold text. Chi-squared degrees of freedom = 2 in all comparisons.

	Predicted group membership					
Taxon	*A. conspersus*	*A. grahami*	*A. opalinus*	Total	χ^2	*P*
Original analysis[a]						
A. conspersus	**48 (100.0%)**	0 (0.0%)	0 (0.0%)	48 (100%)	96.00	<0.0001
A. grahami	2 (4.2%)	**39 (81.3%)**	7 (14.6%)	48 (100%)	50.38	<0.0001
A. opalinus	1 (2.1%)	0 (0.0%)	**47 (97.9%)**	8 (100%)	90.13	<0.0001
Cross-validated[b]						
A. conspersus	**48 (100.0%)**	0 (0.0%)	0 (0.0%)	48 (100%)	96.00	<0.0001
A. grahami	3 (6.3%)	**38 (79.2%)**	7 (14.6%)	48 (100%)	45.88	<0.0001
A. opalinus	1 (2.1%)	0 (0.0%)	**47 (97.9%)**	48 (100%)	90.13	<0.0001

[a] 93.1% of cases in the original analysis were classified correctly to species.

[b] 92.4% of cross-validated cases were classified correctly to species.

To compare the performance of pDFA with DFA, we used the PC scores from two randomly chosen displays of each subject (72 total cases). The pDFA results showed that displays were correctly assigned to species 93.8% of the time in the original analysis (chance level = 51.3%; $P = 0.001$) and 92.5% of the time in the cross-classification analysis (chance level = 47.6%; $P = 0.001$). Both of these results are within one percentage point of the findings for our highest-performing standard DFA.

***Anolis conspersus* populations: Type A displays.**—We ran a PCA on our unit-based variables measured for 16 Type A displays from each of the three *A. conspersus* color morphs. This analysis saved seven rotated PCs that explained 87.5% of the variation in the data (Supplemental Table S26, available online). Weighting of the components on the original variables showed that odd-numbered units (bob durations or standardized peak amplitudes) tended to cluster together and even-numbered units (pause durations) tended to cluster together (Supplemental Table S27, available online). Entering the seven components simultaneously into a DFA produced two discriminant functions (Supplemental Table S28, available online). Four of the components (PC2, PC3, PC6, and PC7) contributed substantially to these functions, with DF1 being most heavily weighted on PC6 (largely Unit 1 duration), and DF2 being most heavily weighted on PC7 (primarily Unit 1 and Unit 3 standardized peak amplitudes; Supplemental Tables S27 and S28). Classification success was high in the original analysis, with 44 of 48 Type A displays (91.7%) being correctly assigned to population (Table 3). Classification success decreased

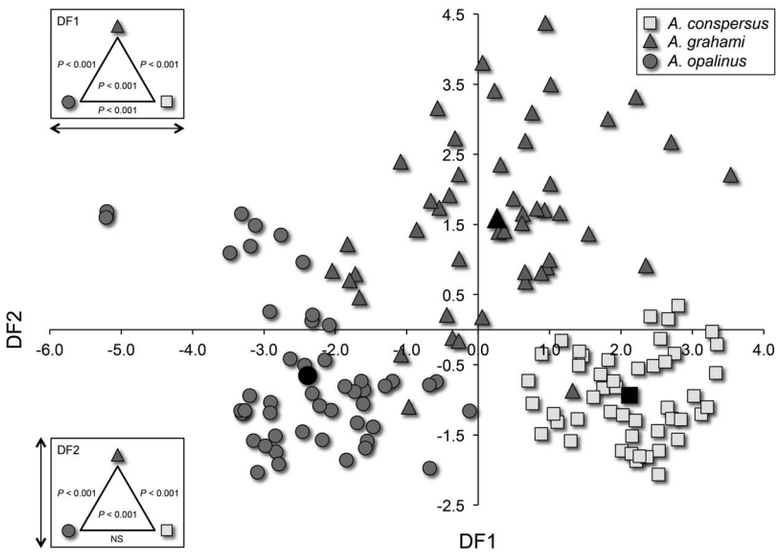

FIG. 21.—Scatterplot of discriminant scores from the two functions generated by a Discriminant Function Analysis (DFA) of *grahami* group species' bobbing displays. The DFA classified principal component (PC) scores derived from unit durations (9 variables) and standardized peak amplitudes (5 variables) in 48 displays from each of the following taxa: (1) squares = *Anolis conspersus* (16 Type A displays from each of the three color morphs), (2) triangles = *A. grahami* (16 Type A displays from *A. g. grahami,* Bermuda; 16 displays unclassified to type from *A. g. grahami,* Discovery Bay, Jamaica; and 16 displays unclassified to type from *A. g. aquarum,* Dragon Bay, Jamaica), and (3) circles = *A. opalinus* (48 displays unclassified to type from a population in Dragon Bay, Jamaica). Distribution centroids for each species are shown as larger black symbols. Insets of triangles in two corners of the plot show the results of Kruskal–Wallis ANOVAs that tested, separately for DF1 and DF2, the null hypothesis that the discriminant scores of the taxa being compared were drawn from the same distribution. The *P*-value shown in the center of each triangle rom the K–W ANOVA of all three taxa. *P*-values adjacent to the sides of each triangle from post hoc pairwise tests indicated by their associated pair of geometric symbols. For exact *P*-values, see Supplemental Table S25. A color version of this figure is available online.

TABLE 3.—Discriminant function analysis of the 7 principal components derived from 15 unit duration/standardized peak amplitude variables used to measure Type A displays in our 3 *A. conspersus* populations. Legend as in Table 2.

	Predicted group membership					
Taxon	*A. c. conspersus* (green morph)	*A. c. lewisi* (brown morph)	*A. conspersus* (blue morph)	Total	χ^2	*P*
Original analysis[a]						
A. c. conspersus	**14 (87.5%)**	0 (0.0%)	2 (12.5%)	16 (100%)	21.50	<0.0001
A. c. lewisi	1 (6.3%)	**15 (93.8%)**	0 (0.0%)	16 (100%)	26.38	<0.0001
A. conspersus (blue)	1 (6.3%)	0 (0.0%)	**15 (93.8%)**	16 (100%)	26.38	<0.0001
Cross-validated[b]						
A. c. conspersus	**13 (81.3%)**	0 (0.0%)	3 (18.8%)	16 (100%)	17.38	0.0002
A. c. lewisi	2 (12.5%)	**12 (75.0%)**	2 (12.5%)	16 (100%)	12.50	0.0019
A. conspersus (blue)	2 (12.5%)	1 (6.3%)	**13 (81.3%)**	16 (100%)	16.63	0.0002

[a] 91.7% of cases in the original analysis were classified correctly to population or subspecies.

[b] 71.2% of cross-validated cases were classified correctly to population or subspecies.

considerably in the cross-validation analysis to 71.2%, with 38 of 48 displays correctly classified (Table 3). Nevertheless, Chi-squared goodness-of-fit tests showed classification success to be greater than chance in all comparisons for both analyses, with misclassifications being roughly equally distributed among the three *A. conspersus* color morphs (Table 3). A scatterplot of discriminant scores showed that DF1 virtually isolated the displays of the green and brown morphs, whereas DF2 was somewhat more effective at separating the displays of the blue morph from those of the other two color morphs (Fig. 22). Kruskal–Wallis ANOVAs showed that discriminant scores differed substantially across the three populations on both axes, and in subsequent Bonferroni-protected pairwise tests DF scores differed between all possible pairings of the three populations except one (Fig. 22, see insets; Supplemental Table S29, available online).

Lower performing DFAs: A DFA run on the combination of unit-based and DFT-based measures performed virtually as well as unit duration/standardized peak amplitude measures alone, with correct classification at 89.6% (43 of 48 displays) in the original analysis and 70.8% (34 of 48 displays) in the cross-validation analysis. Surprisingly, classification of displays using the DFT variables alone was weak in the original analysis at 52.1% (25 of 48 displays) and was very poor in the cross-validation analysis at 35.4% (17 of 48 displays). ?2

Finally, using the PC scores from two randomly chosen displays of each subject (24 total cases), a pDFA correctly assigned displays to species 92.8% of the time in the original analysis (chance level = 76.0%; $P = 0.02$) and 77.5% of the time in the cross-classification analysis (chance level = 58.4%; $P = 0.05$). These results are superior to those of our highest-performing standard DFA for this display type.

***Anolis conspersus* populations: Type B displays.**—We conducted a PCA on the combination of 13 DFT variables and 7 unit duration/standardized peak amplitude variables measured in 16 Type B displays from each of the three *A. conspersus* color morphs. This PCA saved eight rotated PCs that explained 88% of the variation in the data (Supplemental Table S30, available online). The first three components, which accounted for about 47% of the variation, were

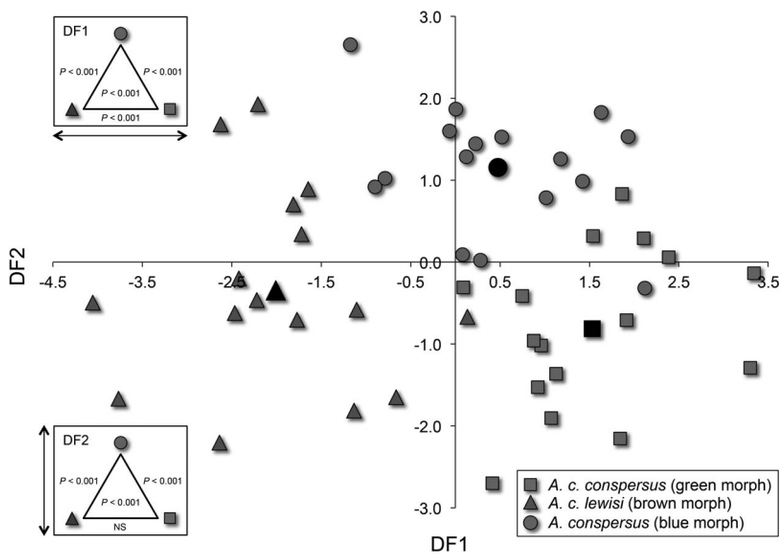

FIG. 22.—Scatterplot of discriminant scores from the two functions generated by a Discriminant Function Analysis (DFA) of Type A bobbing displays from the three *Anolis conspersus* color morphs. The DFA classified principal component (PC) scores derived from unit durations (9 variables) and standardized peak amplitudes (5 variables) in 16 Type A displays from each of the following taxa: (1) squares = *A. c. conspersus* (green morph, George Town), (2) triangles = *A. c. lewisi* (brown morph, East End), and (3) circles = *A. conspersus* (blue morph, West Bay). Legend as in Fig. 21. For exact *P*-values in inset triangles, see Supplemental Table S29. A color version of this figure is available online.

TABLE 4.—Discriminant function analysis of 8 principal components derived from the combination of 13 Discrete Fourier Transform (DFT) variables and 7 unit duration/standardized peak amplitude variables used to measure Type B displays in our 3 *A. conspersus* populations. Legend as in Table 2.

	Predicted group membership					
Taxon	*A. c. conspersus* (green morph)	*A. c. lewisi* (brown morph)	*A. conspersus* (blue morph)	Total	χ^2	*P*
Original analysis[a]						
A. c. conspersus	**12 (75.0%)**	0 (0.0%)	4 (25.0%)	16 (100%)	14.00	0.0009
A. c. lewisi	0 (0.0%)	**15 (93.8%)**	1 (6.3%)	16 (100%)	26.38	<0.0001
A. conspersus (blue)	2 (12.5%)	0 (0.0%)	**14 (87.5%)**	16 (100%)	21.50	<0.0001
Cross-validated[b]						
A. c. conspersus	**11 (68.8%)**	0 (0.0%)	5 (31.3%)	16 (100%)	11.38	0.0034
A. c. lewisi	0 (0.0%)	**13 (81.3%)**	3 (18.8%)	16 (100%)	17.38	0.0002
A. conspersus (blue)	2 (12.5%)	0 (0.0%)	**14 (87.5%)**	16 (100%)	21.50	<0.0001

[a] 85.4% of cases in the original analysis were classified correctly to population or subspecies.

[b] 79.2% of cross-validated cases were classified correctly to population or subspecies.

weighted heavily on 10 of the 13 DFT variables (Supplemental Table S31, available online). A DFA of the eight components produced two discriminant functions (Supplemental Table S32, available online). Four of the components (PC1, PC3, PC4, and PC8) contributed substantially to the functions, with DF1 being most strongly weighted on PC4 (largely Unit 1 duration and total display duration), and DF2 being most heavily weighted on PC3 (three DFT variables; Supplemental Tables S31 and S32). Classification success in the original analysis was moderately high, with 41 of 48 displays (85.4%) being correctly assigned to color morph, but was lower in the cross-validation analysis where 38 of 48 (79.2%) of displays were correctly assigned (Table 4). Nevertheless, classification success was greater than chance in all comparisons (Table 4). The largest number of assignment errors in both analyses were due to green morph displays being incorrectly assigned to the blue morph (Table 4). A scatterplot of the discriminant function scores showed that, similar to Type A displays (Fig. 22), DF1 isolated the scores of the green and brown color morphs, whereas DF2 was more effective at separating scores of the blue morph from the other two color morphs (Fig. 23). Kruskal–Wallis ANOVAs revealed that discriminant scores differed among the three *A. conspersus* populations on both axes, and that all Bonferroni-protected pairwise tests between color morphs were significant (Fig. 23; Supplemental Table S33, available online).

Lower performing DFAs: By comparison, a DFA conducted using the 13 DFT variables assigned 36 of 48 displays (75.0%) to the correct *A. conspersus* population in the original analysis. Correct assignment decreased substantially in the cross-validation analysis to 30 of 48 displays (62.5%). A DFA of our seven unit duration/standardized peak amplitude variables (Supplemental Table S7) performed considerably less well, correctly assigning 31 of 48 displays (64.6%) in the original analysis and 27 of 48 displays (56.3%) in the cross-validation analysis.

Last, using the component scores from two randomly chosen displays of each subject (24 cases), a pDFA correctly assigned to population 88.3% of the time in the original analysis (chance level = 77.7%; $P = 0.096$) and 71.4% of the

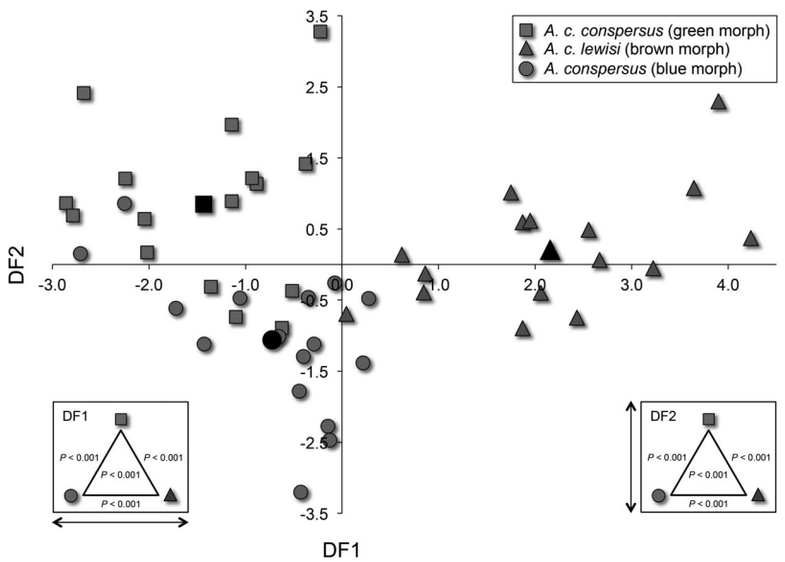

FIG. 23.—Scatterplot of discriminant scores from the two functions generated by a Discriminant Function Analysis (DFA) of Type bobbing displays from the three *Anolis conspersus* color morphs. The DFA classified principal component (PC) scores derived from the combination of 13 Discrete Fourier Transform (DFT) variables plus unit durations (4 variables) and standardized peak amplitudes (3 variables) in 16 Type B displays from each of the following taxa: (1) squares = *A. c. conspersus* (green morph, George Town), (2) triangles = *A. c. lewisi* (brown morph, East End), and (3) circles = *A. conspersus* (blue morph, West Bay). Legend as in Fig. 21. For exact *P*-values in inset triangles, see Supplemental Table S33. A color version of this figure is available online.

TABLE 5.—Discriminant function analysis of 4 principal components derived from the 15 unit duration/standardized peak amplitude variables used to measure displays in our 3 *A. grahami* populations. Legend as in Table 2.

	Predicted group membership					
Taxon	*A. g. grahami* (Bermuda)	*A. g. grahami* (Discovery Bay)	*A. g. aquarium* (Dragon Bay)	Total	χ^2	*P*
Original analysis[a]						
A. grahami grahami[b]	**16 (100.0%)**	0 (0.0%)	0 (00.0%)	16 (100%)	32.00	<0.0001
A. grahami grahami[c]	0 (0.0%)	**15 (93.8%)**	1 (6.3%)	16 (100%)	26.38	<0.0001
A. grahami aquarium	0 (00.0%)	0 (0.0%)	**16 (100.0%)**	16 (100%)	32.00	<0.0001
Cross validated[d]						
A. grahami grahami[b]	**16 (100.0%)**	0 (0.0%)	0 (00.0%)	16 (100%)	32.00	<0.0001
A. grahami grahami[c]	0 (0.0%)	**15 (93.8%)**	1 (6.3%)	16 (100%)	26.38	<0.0001
A. grahami aquarium	0 (00.0%)	1 (6.3%)	**15 (93.8%)**	16 (100%)	26.38	<0.0001

[a] 97.9% of cases in the original analysis were classified correctly to population or subspecies.

[b] Bermuda population (introduced from Kingston, Jamaica).

[c] Discovery Bay population.

[d] 95.8% of cross-validated cases were classified correctly to population or subspecies.

time in the cross-classification analysis (chance level = 54.3%; $P = 0.043$).

***Anolis grahami* populations.**—A PCA of the unit duration/standardized peak amplitude variables measured in 16 displays from each of our three *A. grahami* populations saved 4 rotated PCs. In this analysis PC1 accounted for >31% of the data variation, and together the four components accounted for >85% of the total variation (Supplemental Table S34, available online). Component weighting of the variables revealed that bob unit durations clustered together as did pause unit durations (Supplemental Table S35, available online). A DFA of the four PCs produced two discriminant functions (Supplemental Table S36, available online). Classification success in the original analysis was exceptional, with 47 of 48 (97.9%) displays being correctly assigned to population (Table 5). Classification success in the cross-validation analysis was only one display less successful, with 46 of 48 (95.8%) of displays being correctly assigned. The very few incorrect assignments occurred between the Discovery Bay population of *A. g. grahami*, and *A. g. aquarum* (Table 5; Fig. 24), as could be predicted by the similarity of unit durations and standardized peak amplitudes in these two populations. Kruskal–Wallis ANOVAs showed that discriminant scores differed among the three *A. grahami* populations on both axes, and that all pairwise tests between populations were significant (Fig. 24; Supplemental Table S37, available online).

Lower performing DFAs: A DFA on the combination of DFT-based and unit-based variables produced identical classification success to the unit-based analysis alone, but extracted eight PCs—twice as many as the unit-based analysis. Despite explaining more total variation (89.11% as compared with 85.34% in the unit-based analysis), this improvement did not translate into greater classification success. A DFA carried out on the DFT variables alone performed less well, correctly classifying 43 of 48 displays (87.5%) in the original analysis and 37 of 48 displays in the cross-validation analysis (77.1%).

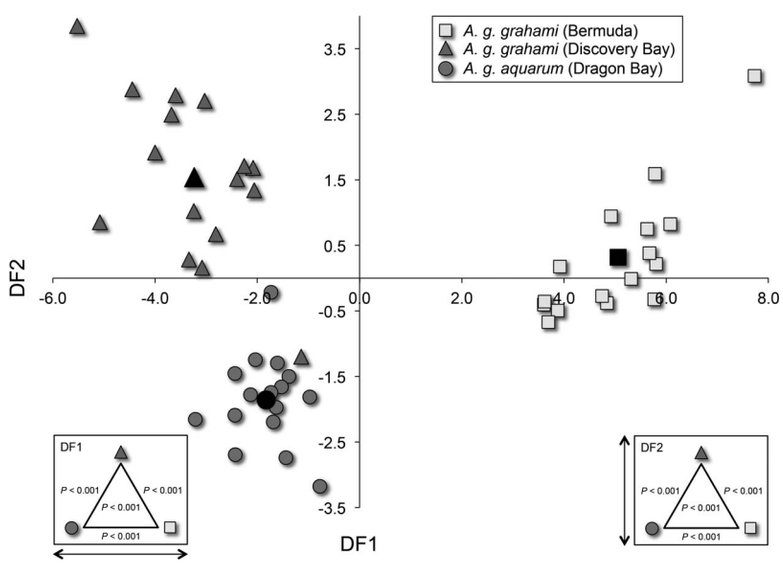

FIG. 24.—Scatterplot of discriminant scores from the two functions generated by a Discriminant Function Analysis (DFA) of bobbing displays from the three *Anolis grahami* populations. The DFA classified principal component (PC) scores derived from unit durations (9 variables) and standardized peak amplitudes (5 variables) in 16 Type A displays from each of the following taxa: squares = *A. g. grahami* (Bermuda), triangles = *A. g. grahami* (Discovery Bay, Jamaica), and circles = *A. g. aquarum* (Dragon Bay, Jamaica). Legend as in Fig. 21. For exact *P*-values in inset triangles, see Supplemental Table S37. A color version of this figure is available online.

TABLE 6.—Discriminant function analysis of 5 principal components derived from the 13 Discrete Fourier Transform (DFT) variables used to measure displays in 3 *A. lineatopus* subspecies. Legend as in Table 2.

	Predicted group membership					
Taxon	*A. l. ahenobarbus*	*A. l. lineatopus*	*A. l. merope*	Total	χ^2	*P*
Original analysis[a]						
A. l. ahenobarbus	**11 (68.8%)**	5 (31.3%)	0 (0.0%)	16 (100%)	11.38	0.0034
A. l. lineatopus	2 (12.5%)	**14 (87.5%)**	0 (0.0%)	16 (100%)	21.50	<0.0001
A. l. merope	1 (6.3%)	0 (0.0%)	**15 (93.8%)**	16 (100%)	26.38	<0.0001
Cross-validated[b]						
A. l. ahenobarbus	**10 (62.5%)**	5 (31.3%)	1 (6.3%)	16 (100%)	7.63	0.0220
A. l. lineatopus	3 (18.8%)	**13 (81.3%)**	0 (0.0%)	16 (100%)	17.38	0.0002
A. l. merope	1 (6.3%)	0 (0.0%)	**15 (93.8%)**	16 (100%)	26.38	<0.0001

[a] 83.3% of cases in the original analysis were classified correctly to subspecies.

[b] 79.2% of cross-validated cases were classified correctly to subspecies.

Finally, using the PC scores from two randomly chosen displays of each subject (24 cases), a pDFA correctly assigned displays to species 98.0% of the time in the original analysis (chance level = 60.6%; $P = 0.002$) and 94.6% of the time in the cross-classification analysis (chance level = 49.0%; $P = 0.002$). These results are virtually identical to those obtained in the highest performing standard DFAs.

***Anolis lineatopus* subspecies.**—A PCA on our DFT variables saved five rotated components, the first of which explained >30% of the variation in the data and the sum of which explained >88% of the variation (Supplemental Table S38, available online). Although Principal Frequency (PrincFreq) was among the five heavily weighted variables comprising PC1, no pattern among the four other variables chosen was apparent (Supplemental Table S39, available online). A DFA on the five components produced two discriminant functions, to which PC1, PC2, and PC4 contributed substantially (Supplemental Table S40, available online). Classification success was moderately high in the original analysis, with 40 of 48 displays (83.3%) being assigned to the correct *A. lineatopus* subspecies. Successful classification was slightly lower in the cross-validation analysis, where 38 of 48 displays (79.2%) were correctly assigned to subspecies (Table 6; Fig. 25). Kruskal–Wallis ANOVAs showed that discriminant scores differed among the three *A. lineatopus* subspecies on both discriminant axes, but results of pairwise comparisons differed in magnitude (Fig. 25, see insets; Supplemental Table S41, available online).

Last, using PC scores from two randomly chosen displays of each subject (24 cases), pDFA correctly assigned displays to subspecies 84.9% of the time in the original analysis (chance level = 65.8%; $P = 0.027$) and 74.4% of the time in the cross-classification analysis (chance level = 50.3%; $P = 0.011$). Compared with the standard DFAs, results of the pDFAs were slightly higher in the original analysis and ≈ 5% lower in the cross-classification analysis.

DFT Performance and Display Types of Differing Structural Complexity

Finally, we tested a hypothesis from Macedonia et al. (2019) that the ability of DFT variables to effectively

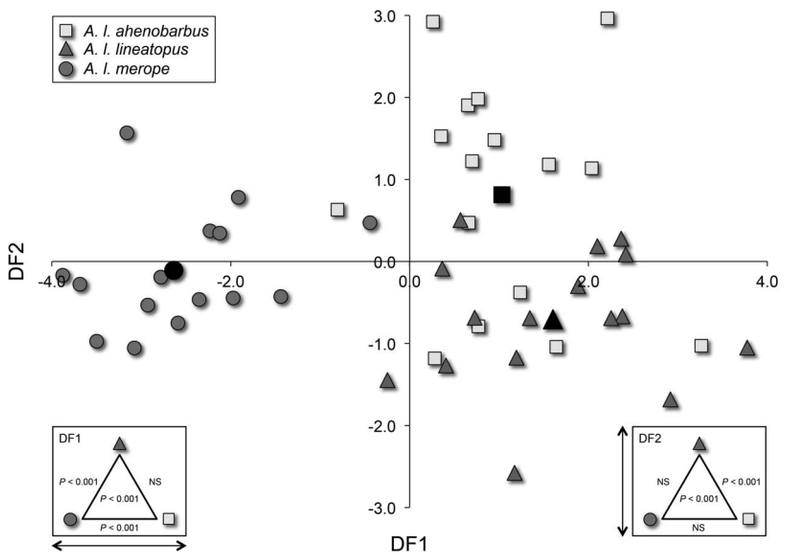

FIG. 25.—Scatterplot of discriminant scores from the two functions generated by a Discriminant Function Analysis (DFA) of bobbing displays from the three *Anolis lineatopus* study populations. The DFA classified principal component (PC) scores derived from 13 Discrete Fourier Transform (DFT) variables in 16 displays from each of the following subspecies: squares = *A. l. ahenobarbus* (Dragon Bay, Jamaica), triangles = *A. l. lineatopus* (Kingston, Jamaica), and circles = *A. l. merope* (Discovery Bay, Jamaica). Legend as in Fig. 21. For exact *P*-values in inset triangles, see Supplemental Table S41. A color version of this figure is available online.

describe bobbing displays may decrease with increasing display complexity. For this test we used four *A. reconditus* display types: two with comparatively simple structure (Types B_2 and B_4) and two with more complex (compound) structure (Types B_2+A and B_4+A; Figs. 13, 14). We acknowledge that the +A display variants are longer in duration than the same displays without Type A units appended (medians: $B_2 = 0.33$ s; B_2+A = 1.00 s; $B_4 = 0.93$ s; B_4+A = 2.30 s; $n = 6$ for each display type). A PCA extracted five components that explained 90.7% of the variation (including or excluding Principal Frequency had no effect on the results). Discriminant function analysis classification success was very high in the original analysis at 95.8%, with B_2, B_2+A, and B_4 displays each being classified at 100%. The only incorrect assignment was of a B_4+A display to B_2+A. Moreover, the cross-validation analysis exhibited only one additional misclassification (91.7% overall success), with two B_4+A displays being incorrectly assigned to B_2+A. The very low error rate in these analyses provides only minimal (and in our view, equivocal) support for our hypothesis (Macedonia et al. 2019) that DFT-based measures of bobbing displays may perform less well as displays become more complex in structure.

Discussion

Evolution of Bobbing Display Structure in the *Grahami* Series Anoles

In this study we used multiple approaches to the description and analysis of bobbing displays in the *grahami* series (*Placopsis*) clade of anoles endemic to Jamaica and Grand Cayman. For most species we found display structure to be moderately to highly stereotyped, because most unit-based measures satisfied Barlow's (1977) criterion for behavioral stereotypy by having CVs below 35%. Among our important results, several species exhibited derived display forms that could not be predicted from the display repertoires of more basal species in the radiation (Fig. 26). For example, although most members of the *grahami* group possess a simple display structure consisting of spike-shaped bobs, the Type B display of *A. conspersus* has no structural equivalent in the *grahami* series and must have evolved after the divergence of *A. conspersus* and *A. grahami*. In contrast, the *A. conspersus* Type A display reveals this species' uniquely shared ancestry with a particular population of *A. grahami*. In this case, the first unit in the display exhibits a derived spike + plateau bob shape otherwise observed only in *A. g. grahami* from southern and central Jamaica, whereas the remaining bobs exhibit the spike shape that appears to be ancestral for the species group (Macedonia and Clark 2001). Phylogeny reconstruction using mtDNA sequence data confirmed that *A. conspersus* is far more closely related to *A. g. grahami* from Kingston (southeastern Jamaica) than to populations from Discovery Bay or Negril (Jackman et al. 2002). Accordingly, molecular clock estimates placed a divergence time of 2.6 mya for *A. conspersus* and Kingston *A. g. grahami*, whereas divergence times between *A. conspersus* and other *A. g. grahami* populations ranged from 7.2 to 7.5 mya (Jackman et al. 2002).

We found the hallmark spike-shaped bobbing displays of most *grahami* group taxa to be absent in the *lineatopus* group. In *A. lineatopus*, displays were highly variable in structure and ranged from brief sinusoidal sequences to volleys of continuously changing bob morphology. Although *A. lineatopus* displays sometimes appeared to contain elements reminiscent of display types in *A. reconditus*, we deemed variation in *A. lineatopus* displays to be too great to assign them to a type. Many *A. lineatopus* displays also included a pause. Jenssen (1977b) found these pauses to be relatively consistent in duration in *A. l. neckeri* displays and he considered them as a link connecting pairs of displays. For two reasons we took a different view. First, pause durations were much more variable in our three subspecies than Jenssen (1977b) found for *A. l. neckeri*. Second, we observed that pauses could occur at any location in a display, as well as in more than one location. The magnitude of variability that we observed in *A. lineatopus* display structure, combined with the difficulty of distinguishing individual displays from display pairs or volleys, led us to include pauses as part of the display in our analyses.

In contrast to *A. lineatopus*, *A. reconditus* exhibited a display repertoire of discrete display types. Phylogenetic analysis has shown that *A. reconditus* is the most basal member of the *lineatopus* group (Figs. 1, 26), with *A. reconditus* and *A. lineatopus* having separated between 9.6 and 9.9 mya (Jackman et al. 2002). Thus, the sinusoidal display morphology and highly variable display structure in our *A. lineatopus* subspecies likely evolved after divergence from *A. reconditus*.

Dewlap display among members of the *grahami* series occurred in two forms: whereas species in the *grahami* group (*A. conspersus*, *A. garmani*, *A. grahami*, and *A. opalinus*) and *A. valencienni* pulsed the dewlap between but not during individual bobbing displays, dewlap pulsing and bobbing appeared to have little temporal relationship to one another during displays in members of the *lineatopus* group (*A. lineatopus* and *A. reconditus*). This finding is consistent with those of Ord et al. (2013), where he considered *A. lineatopus* to be a synchronous displayer (i.e., bobbing and dewlapping occurring largely overlapping in time), and *A. grahami* and *A. opalinus* to be asynchronous displayers (i.e., bobbing and dewlapping exhibit low temporal overlap).

Bobbing Display Structure and Genetic Variation in *A. grahami* Populations

One potential explanation for large subspecific and population differences in *A. grahami* bobbing display structure is that these differences are linked to underlying genetic variation. It is well-established that chromosome number and microstructure are unusually variable in this species ($2n = 30$–37; Blake 1986). Interestingly, Blake (1986) found that chromosome number in *A. g. grahami* from Kingston ($2n = 32$) differed uniformly from that of *A. g. grahami* from Negril ($2n = 36$). Likewise, Jenssen (1981) described considerable population differences in bobbing displays structure of *A. g. grahami* from Kingston and *A. g. grahami* from Negril.

Interestingly, Blake's (1986) Laughland, Jamaica collection site was only 18.4 km east of our Discovery Bay study site (Fig. 2). All but one of her specimens (33 of 34) exhibited a chromosome number of $2n = 34$, which is intermediate between her Kingston and Negril samples. In the present study we found that the flat-topped-spike bob shape in *A. g. grahami* from Discovery Bay also is roughly

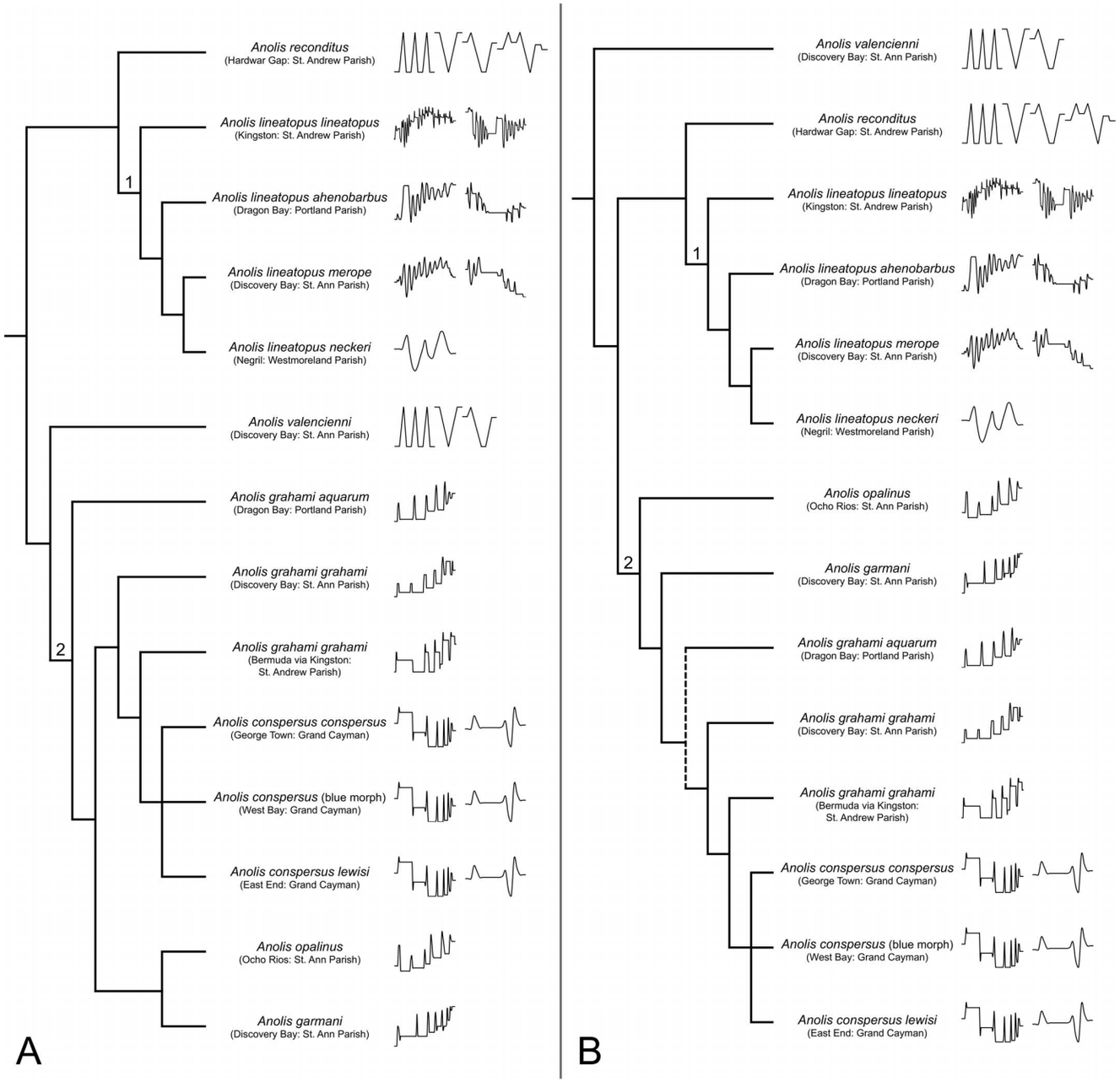

FIG. 26.—Alternative phylogenies of the *grahami* series (*Placopsis*) anoles with corresponding bobbing displays. (A) Phylogenetic hypothesis of Jackman et al. (2002:fig. 4). (B) Phylogenetic hypothesis of Poe et al. (2017: fig. 3), with intraspecific relationships of Jackman et al. (2002). The dashed line indicates that the placement of *A. grahami aquarum* outside an *A. grahami–A. conspersus* clade would violate the species-level results of Poe et al. (2017). The numbers 1 and 2 in the phylogenies indicate the locations of large-scale display structure modifications in the *lineatopus* group and *grahami* group, respectively, contingent on the prospect that the display types shared by *A. reconditus* and *A. valencienni* are homologous. Displays not to scale. Legend as in Fig. 1.

intermediate between the spike + plateau bob shape in *A. g. grahami* from Kingston–Bermuda and the spike bob shape in *A. g. grahami* from Negril (Jenssen 1981).

Why Do *A. reconditus* and *A. valencienni* Share So Many Bobbing Display Types?

Anolis reconditus is a montane generalist that occurs only in the Blue Mountains of Jamaica. This species is the least well known of the *grahami* series (*Placopsis*) anoles as a result of its restricted distribution and mountain isolation (Underwood and Williams 1959; Lazell 1966; Hicks 1973). In contrast, *A. valencienni* is a widespread twig anole that is convergent with other twig anoles in its slender body form, cryptic body color pattern, and creeping movement (Underwood and Williams 1959; Hicks and Trivers 1983; Losos 2009). Despite large ecomorphological and habitat differences, *A. reconditus* and *A. valencienni* uniquely share several bobbing display types that appear to be homologous (Types A, B_1, B_2, and B_3). One potential explanation for the shared displays is that they were present in the common

ancestor of the *grahami* series and were dramatically modified both in the ancestor of *A. lineatopus* (1 in Fig. 26) and in the ancestor of the *grahami* group (2 in Fig. 26). An alternative possibility is that the shared displays types are convergent. Although independent evolution of four display types seems unlikely, these displays are all structurally simple, with display Types B_1, B_2, and B_3 being minor variations on the same theme. A third prospect is that *A. valencienni* is a member of the *lineatopus* group—a phylogeny recovered by Jackman et al. (2002:fig. 6) using the allozymic data of Hedges and Burnell (1990). This finding has not been replicated, however, in more recent DNA-based studies (Pyron et al. 2013; Poe et al. 2017).

Display Variance Within and Among Subjects, and Among Populations

Nested ANOVAs showed that, with the exception of *A. grahami,* within-subject variance was the largest source of variation in display structure for the unit-based and DFT-based variable sets. In *A. grahami,* among-population variance accounted for most of the variation in unit durations and DFT measures. Our Bermuda *A. g. grahami* population performed comparatively quick displays of spike + plateau shaped bobs, where Unit 1 exhibited a much greater duration than subsequent bobs and pauses between bobs were brief. In contrast, our Discovery Bay *A. g. grahami* population produced slower displays of flat-topped-spike bobs that were all similar in duration, and pauses between bobs were comparatively long (particularly Unit 4). Last, our *A. g. aquarum* population exhibited very quick displays consisting entirely of spike-shaped bobs. In this subspecies all bobs were similar in duration, with pauses being either more brief than, or intermediate in duration to, those of the other two populations.

DFA Classification Success of Unit-based and DFT-based Variables

Our inaugural use of the DFT to quantify bobbing displays in Galápagos Lava Lizards (Macedonia et al. 2019) led us to anticipate that this method would be a useful addition to, or might even replace, unit-based display measures for describing motion displays of lizards. In the present study, by comparing classification success in DFAs of unit-based variables, DFT-based variables, and the combination of the two kinds of measures, we discovered that DFT does not provide a panacea in the analysis of bobbing displays. For example, in cross-validation DFAs of Type A displays in our three *A. conspersus* populations, classification success was substantially better for unit-based variables than DFT-based variables or the combination of the two variable sets. However, for *A. conspersus* Type B displays, the combination of the two methods outperformed either method alone. We speculate that fewer unit-based variables measured in *A. conspersus* Type B displays (7 variables) than in Type A displays (15 variables) may have rendered the DFT more valuable for classifying displays to the correct population. In cross-validation DFAs of our three *A. grahami* populations, unit-based variables and the combination of the two variable sets performed identically well, whereas DFT-based variables alone were less successful. These results make clear that one variable set did not consistently outperform another. Rather, the success of each DFA likely depended on within-taxon variation relative to among-taxon variation in the groups being compared.

DFT Performance and Display Types of Differing Structural Complexity

We conducted a preliminary test of a hypothesis that DFT-based variables may perform less effectively as display structure becomes increasingly complex. This hypothesis arose from our finding that DFA classification success of Galápagos Lava Lizard bobbing displays was substantially lower for species with relatively complex displays compared with species with relatively simple displays (Macedonia et al. 2019). Unfortunately, we consider the results of our hypothesis test on *A. reconditus* simple and compound displays to be inconclusive. One misclassification of an *A. reconditus* compound display (B_4+A assigned to B_2+A), and one additional misclassification of the same type in cross-validation, provided only weak support for the hypothesis. We are optimistic, however, that a definitive test of this structural complexity hypothesis can be achieved using synthetic displays that vary in attributes such as bob shape, duration, spacing, uniformity, frequency, and amplitude.

We also had anticipated from Macedonia et al. (2019) that Principal Frequency would be an important DFT variable for capturing taxon-specific attributes of bobbing displays, given that this variable describes the most prominent trigonometric function characterizing display structure. In the present study, results of PCA–DFA analyses that included DFT measures indeed revealed Principal Frequency to be among the most heavily weighted variables comprising the most influential principal component (PC1).

Step-Bobbing: What Is Its Function?

Finally, we recorded step-bobbing displays from four of our seven study species: *A. conspersus, A. grahami, A. lineatopus,* and *A. reconditus*. Jenssen (1979a) already had described step-bobbing in *A. opalinus,* so the only remaining species in the *grahami* series for which step-bobbing has not been noted are *A. garmani* and *A. valencienni*. The ubiquity of step-bobbing in the *grahami* series makes it likely, however, that all species in the clade perform this display.

The function of step-bobbing baffled Jenssen (1979a) and proved equally elusive to us. Jenssen reported step-bobbing in male *A. opalinus* to occur in the apparent absence of conspecifics, to be directed at an observable distant male or female, to be directed at a male in close proximity, and even to be directed toward congeners. We observed that step-bobbing sometimes was alternated irregularly with other bobbing displays, and on occasion it was the only display type that we recorded from a subject. Moreover, step-bobbing in many cases was accompanied with aggressive signals (crest erection, gorged throat, lateral presentation, head tilt toward opponent; Macedonia and Stamps 1994), whereas at other times it was performed in nonagonistic contexts. Despite our observations in *A. grahami* and *A. lineatopus* of step-bobbing co-occurring with aggression, it seems possible that this form of bobbing may function as an appeasement display (Crews 1975; Ord and Evans 2002; Martins and Lacy 2004; Van Dyk and Evans 2008; Vicente 2018) geared toward de-escalating or terminating aggression. We suggest that employing robotic anoles in an interactive experiment (Macedonia et al. 2013, 2015a; Clark et al. 2019) would be an ideal means to

test the appeasement function hypothesis for this enigmatic display.

Acknowledgments.—On Jamaica we thank A. Donaldson, F. McDonald, and Y. Strong of the Natural Resources Conservation Authority, Kingston, as well as J. Woodley (Director), M. Haley (Director), I. Sandeman (Acting Director), and P. Gayle (Principal Scientific Officer) of the Discovery Bay Marine Laboratory (University of the West Indies) for support to collect and export anoles under their general collection permit. On Grand Cayman we thank A. Benjamin, Chief Agriculture and Veterinary Officer, Department of Agriculture, for authorizing export of *A. conspersus*. On Bermuda we thank Government Veterinary Officers N. Burnie and J. Nisbett for permits to collect and export *A. grahami*. We are grateful to I. Maayan and J. Stroud for providing SVL data on the *grahami* series anoles. Numerous undergraduate students from Alma College (Michigan) and Florida Southern College (Florida) aided in the collection of anoles in the field and their maintenance in captivity over the years during which this and related studies took place. We offer a special thanks to S. Echternacht for contributing his time, knowledgeable advice, and lizard noosing skills on Jamaica and Grand Cayman, and for his dependable enthusiasm as this research developed throughout the 1990s and 2000s. The display shown as Fig. 16B is from the first 20 s of a video of *A. valencienni* by T. Ord, available at https://www.youtube.com/watch?v=-ofxOlbBTtw. All supplemental materials for this paper are available at www.macedonialab.com.

Supplemental Material

Supplemental material associated with this article can be found online.

Tables S1–S41.—Available online at https://dx.doi.org/10.1655/HERPMONOGRAPHS-D-20-00007.T1

Video SV1.—*Anolis conspersus conspersus* (green morph male) Type A display volley. Available online at https://dx.doi.org/10.1655/HERPMONOGRAPHS-D-20-00007.V1

Video SV2.—*Anolis conspersus conspersus* (green morph male) Type B display volley. Available online at https://dx.doi.org/10.1655/HERPMONOGRAPHS-D-20-00007.V2

Video SV3.—*Anolis conspersus conspersus* (green morph male) two Type B display volleys. Available online at https://dx.doi.org/10.1655/HERPMONOGRAPHS-D-20-00007.V3

Video SV4.—*Anolis conspersus conspersus* (green morph male) step-bobbing display. Available online at https://dx.doi.org/10.1655/HERPMONOGRAPHS-D-20-00007.V4

Video SV5.—*Anolis conspersus lewisi* (brown morph male) Type A display volley. Available online at https://dx.doi.org/10.1655/HERPMONOGRAPHS-D-20-00007.V5

Video SV6.—*Anolis conspersus lewisi* (brown morph male) Type B display volley. Available online at https://dx.doi.org/10.1655/HERPMONOGRAPHS-D-20-00007.V6

Video SV7.—*Anolis conspersus* (blue morph male) Type A display volley. Available online at https://dx.doi.org/10.1655/HERPMONOGRAPHS-D-20-00007.V7

Video SV8.—*Anolis conspersus* (blue morph male) Type B display volley. Available online at https://dx.doi.org/10.1655/HERPMONOGRAPHS-D-20-00007.V8

Video SV9.—*Anolis garmani* male Type B display. Available online at https://dx.doi.org/10.1655/HERPMONOGRAPHS-D-20-00007.V9

Video SV10.—*Anolis grahami aquarum* males bobbing and step-bobbing displays. Available online at https://dx.doi.org/10.1655/HERPMONOGRAPHS-D-20-00007.V10

Video SV11.—Bermuda *Anolis grahami grahami* males bobbing displays. Available online at https://dx.doi.org/10.1655/HERPMONOGRAPHS-D-20-00007.V11

Video SV12.—Bermuda *Anolis grahami grahami* male step-bobbing display. Available online at https://dx.doi.org/10.1655/HERPMONOGRAPHS-D-20-00007.V12

Video SV13.—*Anolis grahami grahami* male (Discovery Bay) display. Available online at https://dx.doi.org/10.1655/HERPMONOGRAPHS-D-20-00007.V13

Video SV14.—*Anolis grahami grahami* male (Discovery Bay) two displays. Available online at https://dx.doi.org/10.1655/HERPMONOGRAPHS-D-20-00007.V14

Video SV15.—*Anolis lineatopus ahenobarbus* male display. Available online at https://dx.doi.org/10.1655/HERPMONOGRAPHS-D-20-00007.V15

Video SV16.—*Anolis lineatopus lineatopus* male #1 display. Available online at https://dx.doi.org/10.1655/HERPMONOGRAPHS-D-20-00007.V16

Video SV17.—*Anolis lineatopus lineatopus* male #2 display. Available online at https://dx.doi.org/10.1655/HERPMONOGRAPHS-D-20-00007.V17

Video SV18.—*Anolis lineatopus lineatopus* male #3 display. Available online at https://dx.doi.org/10.1655/HERPMONOGRAPHS-D-20-00007.V18

Video SV19.—*Anolis lineatopus lineatopus* male step-bobbing display. Available online at https://dx.doi.org/10.1655/HERPMONOGRAPHS-D-20-00007.V19

Video SV20.—*Anolis lineatopus merope* male display. Available online at https://dx.doi.org/10.1655/HERPMONOGRAPHS-D-20-00007.V20

Video SV21.—*Anolis lineatopus merope* male step-bobbing display. Available online at https://dx.doi.org/10.1655/HERPMONOGRAPHS-D-20-00007.V21

Video SV22.—*Anolis opalinus* male display volley (5 displays). Available online at https://dx.doi.org/10.1655/HERPMONOGRAPHS-D-20-00007.V22

Video SV23.—*Anolis reconditus* female Type B2 and B4 displays. Available online at https://dx.doi.org/10.1655/HERPMONOGRAPHS-D-20-00007.V23

Video SV24.—*Anolis reconditus* male Type B4+A displays. Available online at https://dx.doi.org/10.1655/HERPMONOGRAPHS-D-20-00007.V24

Video SV25.—*Anolis valencienni* male Type B2 displays. Available online at https://dx.doi.org/10.1655/HERPMONOGRAPHS-D-20-00007.V25

Literature Cited

Andersson, M. 1994. Sexual Selection. Princeton University Press, USA.

Barlow, G.W. 1977. Modal action patterns. Pp. 98–134 in How Animals Communicate (T.A. Sebeok, ed.). Indiana University Press, USA.

Blake, J.A. 1986. Complex chromosomal variation in natural populations of the Jamaican lizard *Anolis grahami*. Genetica 69:3–17.

Bradbury, J.W., and S.L. Vehrencamp. 2011. Principles of Animal Communication, 2nd edition. Sinauer Associates, USA.

Caro, T.M. 2005. Antipredator Defenses in Birds and Mammals. The University of Chicago Press, USA.

Carpenter, C.C. 1962. Patterns of behavior in two Oklahoma lizards. American Midland Naturalist 67:132–151.

Carpenter, C.C., and G.W. Ferguson. 1977. Variation and evolution of stereotyped behavior in reptiles. Pp. 335–554 in Biology of the Reptilia, Volume 7: Ecology and Behaviour, A (C. Ganz and D.W. Tinkle, eds.). Academic Press, USA.

Carpenter, C.C., and G.G. Grubitz, III. 1961. Time-motion study of a lizard. Ecology 42:199–200.

Carpenter, C.C., J.A. Badham, and B. Kimble. 1970. Behavior patterns of three species of *Amphibolurus* (Agamidae). Copeia 1970:497–505.

Clark, D.L., J.M. Macedonia, J.W. Rowe, M.A. Stuart, D.J. Kemp, and T.J. Ord. 2015. Evolution and discrimination of species-typical displays in Galápagos lava lizards: Comparative analyses of signalers and robot playbacks to receivers. Animal Behaviour 109:33–34.

Clark, D.L., J.M. Macedonia, J.W. Rowe, K. Kamp, and C.A. Valle. 2017. Responses of Galápagos lava lizards (*Microlophus bivittatus*) to

manipulation of female nuptial coloration on lizard robots. Herpetologica 73:323–330.

Clark, D.L., J.M. Macedonia, J.W. Rowe, M.R. Austin, I.M. Centurione, and C.A. Valle. 2019. Galápagos lava lizards (*Microlophus bivittatus*) respond dynamically to displays from interactive conspecific robots. Behavioral Ecology and Sociobiology 73:136.

Clutton-Brock, T.H., and S.D. Albon. 1979. The roaring of red deer and the evolution of honest advertisement. Behaviour 69:145–170.

Cooper, W.E., Jr., V. Pérez-Melado, T.A. Baird, J.P. Caldwell, and L.J. Vitt. 2004. Pursuit deterrent signaling by the Bonaire whiptail lizard *Cnemidophorus murinus*. Behaviour 141:297–311.

Crews, D. 1975. Inter- and intraindividual variation in display patterns in the lizard *Anolis carolinensis*. Herpetologica 31:37–47.

DeCourcy, K.R., and T.A. Jenssen. 1994. Structure and use of male territorial headbob signals by the lizard *Anolis carolinensis*. Animal Behaviour 47:251–262.

Ferguson, G.W. 1971. Variation and evolution of the push-up displays of the side-blotched lizard genus *Uta* (Iguanidae). Systematic Biology 20:79–101.

Fleishman, L.J., M. Leal, and M.H. Persons. 2009. Habitat light and dewlap color diversity in four species of Puerto Rican anoline lizards. Journal of Comparative Physiology A 195:1043–1060.

Gaetano, J. 2013. Holm–Bonferroni sequential correction: An Excel calculator, Version 1.3. Available at https://www.researchgate.net/publication/322569220_Holm-Bonferroni_sequential_correction_An_Excel_calculator_13. Earlier version archived by WebCite at http://www.webcitation.org/6RgJhQr3J on 8 August 2014.

Gorman, G.C. 1968. The relationships of *Anolis* of the *Roquet* species group (Sauria: Iguanidae). III. Comparative study of display behavior. Breviora 284:1–31.

Grant, C. 1940. The herpetology of the Cayman Islands. Bulletin of the Institute of Jamaica, Science Series 2:1–65.

Hasson, O., R. Hibbard, and G. Ceballos. 1989. The pursuit deterrent function of tail-wagging in the zebra-tailed lizard (*Callisaurus draconoides*). Canadian Journal of Zoology 67:1203–1209.

Hedges, S.B., and K.L. Burnell. 1990. The Jamaican radiation of *Anolis* (Sauria: Iguanidae): An analysis of relationships and biogeography using sequential electrophoresis. Caribbean Journal of Science 26:31–44.

Hicks, R. 1973. New studies on a montane lizard of Jamaica, *Anolis reconditus*. Breviora 404:1–23.

Hicks, R.A., and R.L Trivers. 1983. The social behavior of *Anolis valencienni*. Pp. 570–595 in Advances in Herpetology and Evolutionary Biology: Essays in Honor of Ernest E. Williams (A.G.J. Rhodin and K. Miyata, eds.). Harvard University, USA.

Jackman, T.R., D.J. Irschick, K. de Queiroz, J.B. Losos, and A. Larson. 2002. Molecular phylogenetic perspective on evolution of lizards of the *Anolis grahami* series. Journal of Experimental Zoology 294:1–16.

Jenssen, T.A. 1977a. Evolution of anoline lizard display behavior. American Zoologist 17:203–215.

Jenssen, T.A. 1977b. Morphological, behavioral and electrophoretic evidence of hybridization between the lizards, *Anolis grahami* and *Anolis lineatopus neckeri*, on Jamaica. Copeia 1977:270–278.

Jenssen, T.A. 1978. Display diversity in anoline lizards and problems of interpretation. Pp. 268–285 in Behavior and Neurology of Lizards: An Interdisciplinary Conference (N. Greenberg and P.D. Maclean, eds.). National Institutes of Mental Health, USA.

Jenssen, T.A. 1979a. Display modifiers of *Anolis opalinus* (Lacertilia: Iguanidae). Herpetologica 35:21–30.

Jenssen, T.A. 1979b. Display behaviour of male *Anolis opalinus* (Sauria, Iguanidae): A case of weak display stereotypy. Animal Behaviour 27:173–184.

Jenssen, T.A. 1981. Unusual display behavior by *Anolis grahami* from western Jamaica. Copeia 1981:728–733.

Johnson, M.A., E.G. Cook, and B.K. Kircher. 2019. Phylogeny and ontogeny of lizard display behavior. Pp. 259–287 in Behavior of Lizards: Evolutionary and Mechanistic Perspectives (V. Bels and A. Russell, eds.). CRC Press, USA.

Jolliffe, I.T. 2002. Principal Component Analysis, 2nd edition. Springer, USA.

Kolbe, J.J., R.E. Glor, L. Rodríguez Schettino, Chamizo Lara, A. A. Larson, and J.B. Losos. 2004. Genetic variation increases during biological invasion by a Cuban lizard. Nature 431:177–181.

Labra, A., P. Carazo, E. Desfilis, and E. Font. 2007. Agonistic interactions in a *Liolaemus* lizard: Structure of headbob displays. Herpetologica 63:11–18.

Lazell, J.D., Jr. 1966. Studies on *Anolis reconditus* Underwood and Williams. Bulletin of the Institute of Jamaica, Science Series 18:1–15.

Leal, M. 1999. Honest signalling during prey–predator interactions in the lizard *Anolis cristatellus*. Animal Behaviour 58:521–526.

Losos, J.B. 2009. Lizards in an Evolutionary Tree: Ecology and Adaptive Radiation of Anoles. University of California Press, USA.

Lovern, M.B., T.A. Jenssen, K.S. Orrell, and T. Tuchak. 1999. Comparisons of temporal display structure across contexts and populations in male *Anolis carolinensis*: Signal stability or lability? Herpetologica 55:222–234.

Lowry, R. 2020. VassarStats: Website for Statistical Comparison. Available at http://www.vassarstats.net. Archived by WebCite at http://www.webcitation.org/6Rc2xYZ9h on 5 August 2014.

Macedonia, J.M. 2001. Habitat light, colour variation, and ultraviolet reflectance in the Grand Cayman anole, *Anolis conspersus*. Biological Journal of the Linnean Society 73:299–320.

Macedonia, J.M., and D.L. Clark. 2001. Headbob display analysis of the Grand Cayman anole, *Anolis conspersus*. Journal of Herpetology 35:300–310.

Macedonia, J.M., and D.L. Clark. 2003. Headbob display structure in the naturalized *Anolis* lizards of Bermuda: Sex, context, and population effects. Journal of Herpetology 37:266–276.

Macedonia, J.M., and J.A. Stamps. 1994. Species recognition in *Anolis grahami* (Sauria, Iguanidae): Evidence from responses to video playbacks of conspecific and heterospecific displays. Ethology 98:246–264.

Macedonia, J.M., S. James, L.W. Wittle, and D.L. Clark. 2000. Skin pigments and coloration in the Jamaican radiation of *Anolis* lizards. Journal of Herpetology 34:99–109.

Macedonia, J.M., D.L. Clark, R.G. Riley, and D.J. Kemp. 2013. Species recognition of color and motion signals: Evidence from responses to lizard robots. Behavioral Ecology 24:846–852.

Macedonia, J.M., D.L. Clark, and A.L. Tamasi. 2014. Does selection favor dewlap colors that maximize detectability? A test with five species of Jamaican *Anolis* lizards. Herpetologica 70:157–170.

Macedonia, J.M., D.L. Clark, Z.N. Brown, S. Gensterblum, L. McNabb, A.B. Myrberg, B.D. Myrberg, M.F. Petroche, and A. Karson. 2015a. Responses of *Anolis grahami* males to manipulations of species identity and components of displays in lizard robots. Herpetologica 71:110–116.

Macedonia, J.M., D.L. Clark, L.E. Cherry, N.E. Mohamed, and B.W. Bartel. 2015b. Comparison of headbob displays in gray-dewlapped and red-dewlapped populations of green anoles (*Anolis carolinensis*). Herpetologica 71:117–124.

Macedonia, J.M., D.L. Clark, and A.P. McIntosh. 2016. Differential range expansion and habitat use among the naturalized *Anolis* lizards of Bermuda. Herpetological Review 46:529–535.

Macedonia, J.M., D.L. Clark, M.R. Fonley, I. Centurione, J.W. Rowe, and C.A. Valle. 2019. Analysis of bobbing displays in four species of Galápagos lava lizards using conventional and novel quantitative methods. Herpetologica 75:290–300.

Martins, E. 1993. A comparative study of the evolution of *Sceloporus* push-up displays. The American Naturalist 142:994–1018.

Martins, E.P., and K.E. Lacy. 2004. Behavior and ecology of rock iguanas. I. Evidence for an appeasement display. Pp. 101–108 in Iguanas: Biology and Conservation (A.C. Alberts, R.L. Carter, W.K. Hayes, and E.P. Martins, eds.). University of California Press, USA.

Martins, E.P., and J. Lamont. 1998. Estimating ancestral states of a communicative display: A comparative study of *Cyclura* rock iguanas. Animal Behaviour 55:1685–1706.

Martins, E., A. Labra, M. Halloy, and E.T. Thompson. 2004. Large-scale patterns of signal evolution: An interspecific study of *Liolaemus* lizard headbob displays. Animal Behaviour 68:453–463.

McDonald, J.H. 2014. Handbook of Biological Statistics, 3rd edition. Available at http://www.biostathandbook.com. Sparky House Publishing, USA. Archived by WebCite at http://www. webcitation.org/6RgCVpl4x on 8 August 2014.

Mundry, R. 2015. pDFA User's Manual (informal). Available from the author at roger_mundry@eva.mpg.de.

Mundry, R., and C. Sommer. 2007. Discriminant function analysis with nonindependent data: Consequences and an alternative. Animal Behaviour 74:965–976.

Nicholson, K.E., L.J. Harmon, and J.B. Losos. 2007. Evolution of *Anolis* lizard dewlap diversity. PLOS One 2:e274.

Ord, T.J., and C.S. Evans. 2002. Interactive video playback and opponent assessment in lizards. Behavioural Processes 59:55–65.

Ord, T.J., and E.P. Martins. 2006. Tracing the origins of signal diversity in

anole lizards: Phylogenetic approaches to inferring the evolution of complex behaviour. Animal Behaviour 71:1411–1429.

Ord, T.J., J.A. Stamps, and J.B. Losos. 2013. Convergent evolution in the territorial communication of a classic adaptive radiation: Caribbean *Anolis* lizards. Animal Behaviour 85:1415–1426.

Ord, T.J., D.A. Klomp, J. Garcia-Porta, and M. Hagman. 2015. Repeated evolution of exaggerated dewlaps and other throat morphology in lizards. Journal of Evolutionary Biology 23:1948–1964.

Perez-Martinez, C.A., J.L. Riley, and M.J. Whiting. 2020. Uncovering the function of an enigmatic display: Antipredator behaviour in the iconic Australian frillneck lizard. Biological Journal of the Linnean Society 129:425–438.

Peters, R.A., and C.S. Evans. 2003. Design of the Jacky dragon visual display: Signal and noise characteristics in a complex moving environment. Journal of Comparative Physiology A 189:447–459.

Peterson, C.R. 2016. Color, Color Pattern, Habitat Use, and Morphology of *Anolis conspersus*. Master's thesis, University of Tennessee, USA.

Poe, S., A. Nieto-Montes de Oca, O. Torres-Carvajal, . . . I. Latella. 2017. A phylogenetic, biogeographic, and taxonomic study of all extant species of *Anolis* (Squamata; Iguanidae). Systematic Biology 66:663–697.

Prum, R.O. 1994. Phylogenetic analysis of the evolution of alternative social behavior in the manakins (Aves: Pipridae). Evolution 48:1657–1675.

Pyron, R.A., F.T. Burbrink, and J.J. Wiens. 2013. A phylogeny and revised classification of Squamata, including 4161 species of lizards and snakes. BMC Evolutionary Biology 13:1–53.

R Core Team. 2016. R: A Language and Environment for Statistical Computing, Version 3.3.2. Available at https://www.r-project.org/. R Foundation for Statistical Computing, Austria.

Ramos, J.A., and R.A. Peters. 2017. Motion-based signaling in sympatric species of Australian agamid lizards. Journal of Comparative Physiology A 203:661–671.

Reynolds, R.G., J.J. Kolbe, R.E. Glor, M. López-Darias, C.V. Gómez-Pourroy, A.S. Harrison, K. de Queiroz, L.J. Revell, and J.B. Losos. 2020. Phylogeographic and phenotypic outcomes of brown anole colonization across the Caribbean provide insight into the beginning stages of an adaptive radiation. Journal of Evolutionary Biology 33:468–494.

Schwartz, A., and R.W. Henderson. 1985. A Guide to the Identification of the Amphibians and Reptiles of the West Indies, Exclusive of Hispaniola. Milwaukee Public Museum, USA.

Shine, R. 1990. Function and evolution of the frill of the frillneck lizard, *Chlamydosaurus kingii* (Sauria: Agamidae). Biological Journal of the Linnean Society 40:11–20.

Shochat D., and H.C. Dessauer. 1981. Comparative immunological study of albumins of *Anolis* lizards of the Caribbean islands. Comparative Biochemistry and Physiology 68:67–73.

Stamps, J.A., and G.W. Barlow. 1973. Variation and stereotypy in the displays of *Anolis aeneus* (Sauria: Iguanidae). Behaviour 47:67–94.

Stroud, J.T., and J.B. Losos. 2020. Bridging the process-pattern divide to understand the origins and early stages of adaptive radiation: A review of approaches with insights from studies of *Anolis* lizards. Journal of Heredity 2020:33–42.

Stroud, J.T., S.T. Giery, and M.E. Outerbridge. 2017. Establishment of *Anolis sagrei* on Bermuda represents a novel ecological threat to critically endangered Bermuda skinks (*Plestiodon longirostris*). Biological Invasions 19:1723–1731.

Underwood, G., and E. Williams. 1959. The anoline lizards of Jamaica. Bulletin of the Institute of Jamaica, Science Series 9:1–48.

Van Dyk, D.A., and C.S. Evans. 2008. Opponent assessment in lizards: Examining the effect of aggressive and submissive signals. Behavioral Ecology 19:895–901.

Vicente, N.S. 2018. Headbob displays signal sex, social context and species identity in a *Liolaemus* lizard. Amphibia-Reptilia 39:203–218.

Vicente, N.S. 2019. Arm-wave display in a *Liolaemus* lizard. Herpetological Journal 29:184–188.

Williams, E.E. 1972. The origin of faunas. Evolution of lizard congeners in a complex island fauna: A trial analysis. Pp. 47–89 in Evolutionary Biology (T. Dobzhansky, M.K. Hecht, and W.C. Steer, eds.). Springer, USA.

Williams, E.E. 1983. Ecomorphs, faunas, island size, and diverse endpoints in island radiations of *Anolis*. Pp. 326–370 in Lizard Ecology: Studies of a Model Organism (R.B. Huey, E.R. Pianka, and T.W. Schoener, eds.). Harvard University Press, USA.

Williams, E.E., and A.S. Rand. 1977. Species recognition, dewlap function and faunal size. American Zoologist 17:261–270.

Wingate, D.B. 1965. Terrestrial fauna of Bermuda. Herpetologica 21:202–218.

Accepted on 27 November 2020
Published on Month 2021